



## Pharmacological insights emerging from the characterization of a large collection of synthetic cannabinoid receptor agonists designer drugs

Claudia Gioé-Gallo<sup>a,b</sup>, Sandra Ortigueira<sup>a,b</sup>, José Brea<sup>c,\*</sup>, Iu Raïch<sup>d,e</sup>, Jhonny Azuaje<sup>a,b</sup>, M. Rita Paleo<sup>a</sup>, Maria Majellaro<sup>a,b</sup>, María Isabel Loza<sup>c</sup>, Cristian O. Salas<sup>f</sup>, Xerardo García-Mera<sup>b</sup>, Gemma Navarro<sup>d,e,\*\*</sup>, Eddy Sotelo<sup>a,b,\*\*\*</sup>

<sup>a</sup> Centro Singular de Investigación en Química Biolóxica e Materiais Moleculares (CiQUS), Universidade de Santiago de Compostela, Santiago de Compostela 15782, Spain

<sup>b</sup> Departamento de Química Orgánica, Facultad de Farmacia, Universidade de Santiago de Compostela, Santiago de Compostela 15782, Spain

<sup>c</sup> Centro Singular de Investigación en Medicina Molecular y Enfermedades Crónicas (CiMUS), Universidade de Santiago de Compostela, Santiago de Compostela 15782, Spain

<sup>d</sup> Department of Biochemistry and Physiology, School of Pharmacy and Food Science, Universitat de Barcelona, Barcelona 08028, Spain

<sup>e</sup> Institute of Neurosciences (NeuroUB), Campus Mundet, University of Barcelona, Barcelona 08035, Spain

<sup>f</sup> Department of Organic Chemistry, Faculty of Chemistry and Pharmacy, Pontificia Universidad Católica de Chile, Vicuña Mackenna 4860, Macul, Santiago 7820436, Chile

### ARTICLE INFO

#### Keywords:

Synthetic cannabinoid receptor agonists  
SCRAs  
Synthetic cannabinoids NPS  
Abuse drugs  
Designer drugs  
CB<sub>1</sub>  
CB<sub>2</sub>  
Cannabinoids  
Indole  
Indazole

### ABSTRACT

Synthetic cannabinoid receptor agonists (SCRAs) constitute the largest and most defiant group of abuse designer drugs. These new psychoactive substances (NPS), developed as unregulated alternatives to cannabis, have potent cannabimimetic effects and their use is usually associated with episodes of psychosis, seizures, dependence, organ toxicity and death. Due to their ever-changing structure, very limited or nil structural, pharmacological, and toxicological information is available to the scientific community and the law enforcement offices. Here we report the synthesis and pharmacological evaluation (binding and functional) of the largest and most diverse collection of enantiopure SCRAs published to date. Our results revealed novel SCRAs that could be (or may currently be) used as illegal psychoactive substances. We also report, for the first time, the cannabimimetic data of 32 novel SCRAs containing an (R) configuration at the stereogenic center. The systematic pharmacological profiling of the library enabled the identification of emerging Structure-Activity Relationship (SAR) and Structure-Selectivity Relationship (SSR) trends, the detection of ligands exhibiting incipient cannabinoid receptor type 2 (CB<sub>2</sub>R) subtype selectivity and highlights the significant neurotoxicity of representative SCRAs on mouse primary neuronal cells. Several of the new emerging SCRAs are currently expected to have a rather limited potential for harm, as the evaluation of their pharmacological profiles revealed lower potencies and/or efficacies. Conceived as a resource to foster collaborative investigation of the physiological effects of SCRAs, the library obtained can contribute to addressing the challenge posed by recreational designer drugs.

### 1. Introduction

New psychoactive substances (NPS), also known as “designer drugs”

or “legal highs” are a broad class of abuse drugs that have emerged on the illicit drug market [1,2]. They are usually conceived by performing structural modifications of existing controlled substances, thereby

**Abbreviations:** NPS, New psychoactive substances; SCRAs, Synthetic cannabinoid receptor agonists; EMCDDA, European Monitoring Centre for Drugs and Drug Addiction; SAR, Structure-activity relationship; SSR, structure-selectivity relationship; GPCRs, G-protein-coupled receptors; CBRs, Cannabinoid receptors; CB1Rs, Cannabinoid 1 receptors; CB2Rs, Cannabinoid 2 receptors; CD, Circular dichroism.

\* Corresponding author.

\*\* Corresponding author at: Department of Biochemistry and Physiology, School of Pharmacy and Food Science, Universitat de Barcelona, Barcelona 08028, Spain.

\*\*\* Corresponding author at: Centro Singular de Investigación en Química Biolóxica e Materiais Moleculares (CiQUS), Universidade de Santiago de Compostela, Santiago de Compostela 15782, Spain.

E-mail addresses: [pepo.brea@usc.es](mailto:pepo.brea@usc.es) (J. Brea), [g.navarro@ub.edu](mailto:g.navarro@ub.edu) (G. Navarro), [e.sotelo@usc.es](mailto:e.sotelo@usc.es) (E. Sotelo).

<https://doi.org/10.1016/j.bioph.2023.114934>

Received 28 December 2022; Received in revised form 1 April 2023; Accepted 22 May 2023

Available online 24 May 2023

0753-3322/© 2023 The Authors. Published by Elsevier Masson SAS. This is an open access article under the CC BY-NC-ND license (<http://creativecommons.org/licenses/by-nc-nd/4.0/>).

mimicking their pharmacological effects, and circumventing governmental legislation [1–3]. NPS are generally grouped into four somewhat overlapping functional categories (according to their chemical structure and pharmacological effects): stimulants, hallucinogens, depressants, and cannabinoids [1,3,4]. NPS provide users with novel alternatives to traditional and well-characterized drugs of abuse (e.g., amphetamines, heroin, cocaine, and cannabis) [4]. They are undergoing a period of proliferation and diversification, with a significant increase in the challenges faced by emergency and critical care physicians, toxicologists, and regulatory governmental authorities [5,6].

Synthetic cannabinoid receptor agonists (SCRAs) have proliferated during the last decade, emerging as the largest and most defiant group of NPS controlled by the European Monitoring Centre for Drugs and Drug Addiction (EMCDDA) [1,4,7]. Initially conceived for therapeutic purposes, SCRAs have become a major public health concern due to their adverse effects, limited safety profile, evolving structure and diversity (Fig. 1) [6–8]. In the middle of the 2000 s, SCRAs entered the abuse drug market in the form of herbal mixtures (e.g., “Spice”, “K2”, “AK-47 24 Karat Gold”). Their use was popularized thanks to their image as a “legal” inexpensive alternative to cannabis (e.g., psychoactive and analgesic effects), which, at the time, was undetectable to routine drug testing [6,7,9]. SCRAs and the main psychoactive component of cannabis [ $\Delta^9$ -tetrahydrocannabinol ( $\Delta^9$ -THC)] do not differ only in their structure, but also qualitatively and quantitatively in their

pharmacological profile [10,11]. [(the former usually being more potent and efficacious as cannabinoid receptor agonists than  $\Delta^9$ -THC which is a partial agonist of both Cannabinoid receptors (CBRs)]. However, in vivo studies have evidenced that SCRAs produce most of the characteristic effects of cannabis consumption in rodents (e.g., hypothermia, bradycardia, catalepsy, hypo-locomotion and antinociception) [4]. It is well documented that SCRAs exert their psychoactive effects through their agonism on the central cannabinoid receptor 1 (CB<sub>1</sub>R) [4,5,8] although they often exhibit a more pronounced agonist effect on cannabinoid receptor 2 (CB<sub>2</sub>R) [4,5,8]. The exception to this trend is a newly emerged SCRA that has been reported to have CB<sub>1</sub>R but not CB<sub>2</sub>R activation potential [12]. CBRs are classical G-protein-coupled receptors (GPCRs), that belong to the large rhodopsin-like class A family [13]. Both CBRs are coupled to G<sub>i</sub> proteins, inhibiting adenylate cyclase and inducing a reduction in the intracellular cyclic adenosine monophosphate (cAMP) levels [14]. CB<sub>1</sub>Rs are one of the most abundant GPCRs in the brain [14,15], also being highly expressed in the peripheral nervous system and other peripheral tissues. In contrast, CB<sub>2</sub>Rs are poorly expressed in brain tissue, being mainly restricted to microglial cells [16]. CB<sub>2</sub>Rs are predominantly expressed in immune cells [17], and are actively implicated in inflammation [18].

The paucity of thorough studies delineating the pharmacology, toxicity, and abuse liability of new SCRAs poses a threat to public health [6,19]. SCRAs consumption has been unequivocally associated with

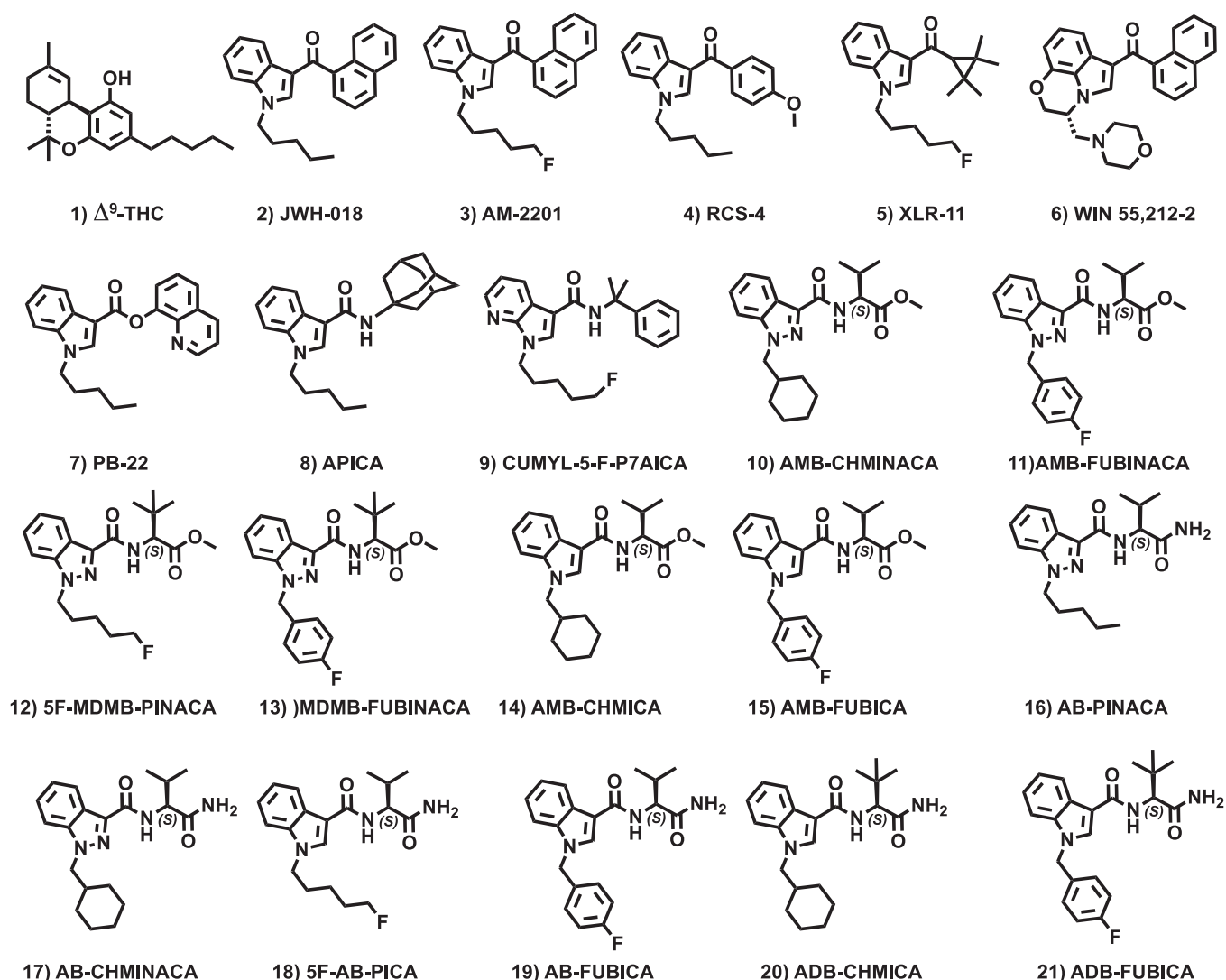


Fig. 1. Structure of  $\Delta^9$ -THC and representative SCRAs [7,20,24,25].

severe adverse effects (e.g., psychosis, delirium, cardiotoxicity, seizures, acute kidney injury, hypothermia), being implicated in numerous deaths in several countries [4,5,9,20,21]. Because many abused SCRA (Fig. 1) are unknown before they are detected by forensic scientists, their effects on humans are poorly or not known at all. [2,19] Likewise, clinical and forensic toxicology laboratories are confronted by analytical challenges when dealing with this family of abuse substances. The huge number and diversity of compounds, their evolving structure and the limited availability of SCRA standards, metabolites and analytical methods complicates these tasks [19,22,23].

Since their early detection on the illicit drug market, [1] SCRA have undergone continuous structural evolution and diversification. Representative structures can be found in Fig. 1. Structural modifications not only affect the central heterobicyclic core, but also involve functional group replacements (ketones, esters, and amides) and diversification of the alkyl chains [5,7,8,21]. The most prevalent chemotypes in SCRA are indole-3-carboxamides and indazole-3-carboxamides featuring pendant amino acid derivatives [5,7,8]. Inspired by early Pfizer patents [26], which claimed synthetic CBR agonists as analgesics, the stereocenter within the pendant amino acid in these compounds is always in the (*S*) configuration [4,21,24,27–29]. Although a recent study explored the role of the stereodisposition of the *iso*-propyl and *tert*-butyl side chains of representative SCRA (Fig. 1), [24] this issue remains unresolved [30]. The evolving structure and limited availability of large SCRA collections by the scientific community has impeded their in-depth characterization from a pharmacological, pharmacokinetic, and toxicological point of view [22]. Several academic groups have generated valuable structural and pharmacological data that sheds light on the complex physiological actions elicited by the SCRA [31,32]. These studies generally focus on the most frequently abused compounds (and their analogues) and usually exclusively evaluate the (*S*) enantiomers, while the corresponding (*R*) stereoisomers remain almost unexplored [7,8,21,24,31]. Moreover, published available pharmacological data of SCRA are usually incomplete. It is well accepted that both the affinity of a drug for its receptor and its ability to produce an effect are important features during ligand characterization and should be determined. Accordingly, there is a demand for large and stereochemically diverse collections of SCRA for detailed characterization to be shared within the scientific community, in a collaborative manner, to unravel the molecular basis of the SCRA physio/toxicological actions. Furthermore, these libraries provide reference standards to forensic laboratories and regulatory authorities [22] thus enabling the fight

against abuse substances by anticipating drugs that might enter the illegal market. In addition, comprehensive SAR data would allow a better understanding of the structural features that govern CBRs activation and their translation into new therapeutic opportunities.

Herein we report the synthesis and pharmacological characterization (at CB<sub>1</sub>R and CB<sub>2</sub>R) of the largest published collection of SCRA (Fig. 2, 64 ligands). The library, which exhibits skeletal, stereochemical and functional diversity, as well as the most frequent alkyl groups at positions R<sup>1</sup> and R<sup>2</sup>, was conceived as a collaborative resource to foster the investigation of the physiological effects of SCRA. The pharmacological profiling (binding affinities and functional data) enabled both the analysis of the most salient features emerging from the structure-activity relationship (SAR) and structure-selectivity relationship (SSR) in these series, and the identification of some CB<sub>2</sub>R selective ligands. We also examined the neurotoxicity of representative SCRA on mouse primary neuronal cells, preliminarily demonstrating a significant neurotoxic effect for some of the frequently abused ligands.

## 2. Materials and methods

### 2.1. Chemistry. General procedure for the synthesis of SCRA 22-25

A mixture of the 1-alkyl-1*H*-indole (or indazole)–3-carboxylic acid (1 mmol), the corresponding amino acid derivative (30 or 31) (1,5 mmol), HATU (1,5 mmol) and DIPEA (4 mmol) in CH<sub>2</sub>Cl<sub>2</sub> (2 mL) was stirred with orbital stirring at room temperature for 24 h. After completion of the reaction, water was added, and the mixture was extracted with CH<sub>2</sub>Cl<sub>2</sub>. The organic phase was dried over MgSO<sub>4</sub>, filtered, and concentrated. The resulting product was purified by column chromatography on silica gel. The purity of all prepared compounds was established by high-performance liquid chromatography (HPLC) and showed to be > 95%. A detailed description of the experimental protocols, equipment and techniques used in the synthesis of targeted ligands, as well as the structural and spectroscopic data obtained for all the compounds described is given in the [Supplementary Information](#).

### 2.2. Circular dichroism (CD)

CD spectra of ligands (>98%) were recorded on a Jasco-815 system equipped with a Peltier-type thermostatic accessory (CDF-426S, Jasco). Measurements were carried out at 20 °C using a 1-mm quartz cell in a volume of 300–350 μL. Compounds (0.1 mg) were dissolved in MeOH

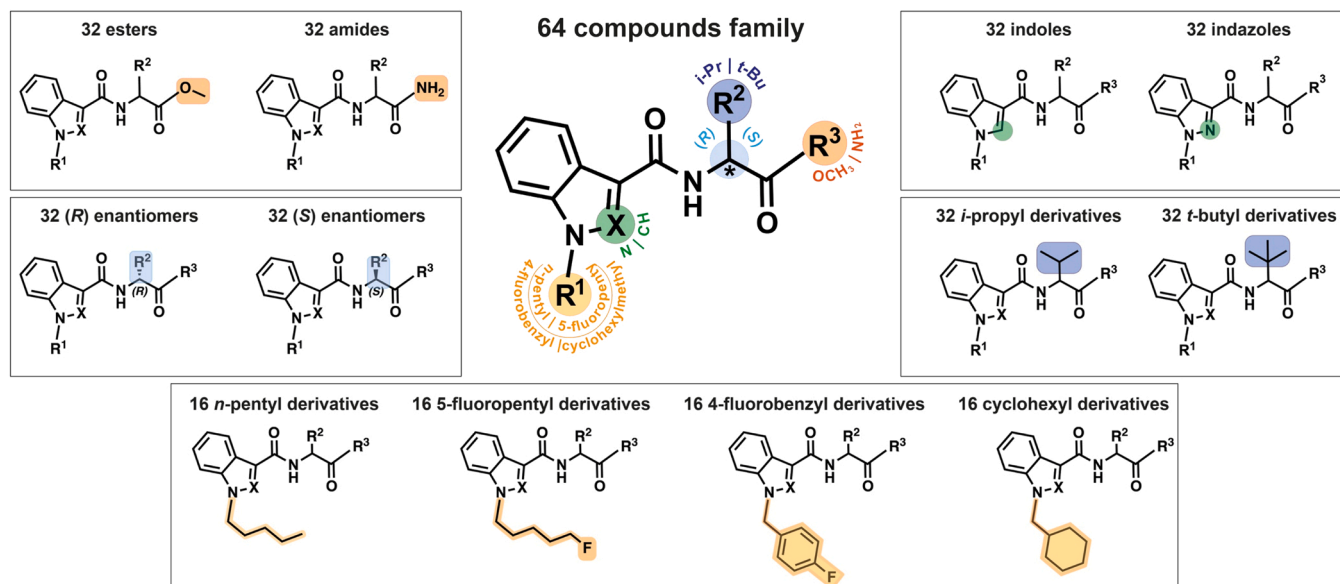


Fig. 2. General structure of the library and diversity elements included.

(1.0 mL). The instrument settings were bandwidth, 1.0 nm; data pitch, 1.0 nm; speed, 500 nm/min; accumulation, 10; wavelengths, 400–190 nm.

### 2.3. Binding assays

Radioligand binding competition assays of CB<sub>1</sub> receptors were carried out in polypropylene 96-well plates by incubating 5 µg of membranes from Chinese hamster ovary (CHO)-CB<sub>1</sub> C3 cell line (PerkinElmer) with 1 nM [<sup>3</sup>H]-CP55940 (Perkin Elmer) and test compounds in binding buffer (50 mM Tris-HCl, 5 mM MgCl<sub>2</sub>, 1 mM EDTA, 0.5% BSA. pH:7,4). Non-specific binding was determined in the presence of 10 µM Surinabant. The reaction mixture was incubated at 30 °C for 60 min, then 200 µL were transferred to GF/C 96-well plate (Millipore, Madrid, Spain) and washed four times with 250 µL wash buffer (50 mM Tris-HCl, 5 mM MgCl<sub>2</sub>, 1 mM EDTA, 0.5% BSA. pH:7,4). Radioactivity was detected in a microplate beta scintillation counter (Microbeta Trilux, PerkinElmer, Madrid, Spain). Radioligand binding competition assays of CB<sub>2</sub> receptors were carried out in polypropylene 96-well plates by incubating 5 µg of membranes from Human embryonic kidney 293 cells (HEK)-CB<sub>2</sub> cell line with 0.2 nM [<sup>3</sup>H]-CP55940 (Perkin Elmer) and test compounds in binding buffer (50 mM Tris-HCl, 5 mM MgCl<sub>2</sub>, 2.5 mM EGTA, 0.1% BSA. pH: 7,4). Non-specific binding was determined in the presence of 10 µM GW405833. The reaction mixture was incubated at 30 °C for 90 min, then 200 µL were transferred to GF/C 96-well plate (Millipore, Madrid, Spain) and washed four times with 250 µL wash buffer (50 mM Tris-HCl, 5 mM MgCl<sub>2</sub>, 2.5 mM EGTA, 1% BSA. pH: 7,4). Data was fitted to 4-parameter logistic equation by employing GraphPad Prism software (V7.0) and K<sub>i</sub> data was calculated with the equation:

$$K_i = IC_{50} / (1 + (F/K_D))$$

where IC<sub>50</sub> was the concentration of the ligand that displaced the specific binding of the radioligand in a 50%; K<sub>D</sub> is the dissociation constant of the radioligand, and F is the concentration of the radioligand employed in the assay.

### 2.4. Functional experiments. Cell Culture and transient transfection

HEK-293 T cells were grown in Dulbecco's Modified Eagle's Medium (DMEM) medium (Gibco, Paisley, Scotland, United Kingdom) supplemented with 2 mM L-glutamine, 100 U/mL penicillin/streptomycin, MEM Non-Essential Amino Acids Solution (1/100) and 5% (v/v) heat inactivated Fetal Bovine Serum (FBS) (Invitrogen, Paisley, Scotland, United Kingdom). Cells were maintained in a humid atmosphere of 5% CO<sub>2</sub> at 37°C. Cells were transiently transfected with the PEI (Polyethyleneimine, Sigma, St. Louis, MO, United States) method as previously described [33] and used for functional assays 48 h later.

### 2.5. Neuronal primary cultures

To prepare primary neurons, brains from fetuses of pregnant CD1 mice were removed (gestational age: 19 days). Neurons were isolated as described in Hradsky et al. [34] Briefly, after removal of the meninges, samples were dissected and digested with 0.25% trypsin (20 min at 37°C). The effect of trypsin was stopped by adding an equal volume of culture medium (supplemented DMEM). A single-cell suspension was obtained by repeated pipetting followed by passage through a 100 µm-pore mesh. Pelleted (7 min, 200g) cells were resuspended in 2 mL of supplemented DMEM and seeded at a density of 3.5 × 10<sup>5</sup> cells/mL in 6-well plates. After 24 h, the medium was replaced by neurobasal medium supplemented with 2 mM L-glutamine, 100 U/mL penicillin/streptomycin and 2% (v/v) B27 medium (GIBCO, Waltham, MA, USA). Primary neurons were assayed after 14 days in culture. Using NeuN as a marker, the percentage of neurons in the

culture was > 90%.

### 2.6. cAMP Determination

Signaling experiments have been performed as previously described. [35] Two hours before initiating the experiment, HEK-293 T cell-culture medium was replaced by serum-starved DMEM medium. Then, cells were detached, resuspended in growing medium containing 50 mM zardaverine (Tocris, Bristol, UK) and placed in 384-well microplates (2500 cells/well). Cells were pretreated (15 min) with cannabinoid compounds (1 nM to 100 µM) -or- vehicle- before adding 0.5 mM forskolin (Tocris, Bristol, UK) to induce cAMP accumulation. Readings were performed after 15 min incubation at 25°C. Homogeneous Time Resolved Fluorescence (HTRF) energy transfer measures were performed using the Lance Ultra cAMP kit (PerkinElmer, Waltham, MA, United States). Fluorescence at 665 nm was analyzed in a PHERA star Flagship microplate reader equipped with an HTRF optical module (BMG Lab Technologies, Offenburg, Germany).

### 2.7. Viability assay

Primary cultures of striatal neurons were treated for 24 h with some representative SCRA (100 nM). Afterwards, cells were scrapped from the plate and resuspended in neurobasal medium supplemented with 2 mM L-glutamine, 100 U/mL penicillin/streptomycin and 2% (v/v) B27 (GIBCO). Trypan blue staining was performed mixing 1 part of 0.4% trypan blue and 1 part of cell suspension in a plastic tube. After ~3 min of incubation at room temperature, 10 µL of the mixture were sampled in a Neubauer chamber and counted with a Countess II FL (Life Technologies, California, CA, USA). The unstained (viable) and stained (nonviable) cells were counted separately, and the percentage of viability was calculated as: total number of viable cells/total number of cells x 100.

### 2.8. Data and statistical analysis

K<sub>i</sub> and EC<sub>50</sub> values were obtained by fitting the data with nonlinear regression using Prism 9 software (GraphPad, San Diego, CA). Results are the mean of four experiments (n = 4), each performed in duplicate. Data are represented as mean ± standard error of mean (SEM) with statistical significance set at P < 0.05. The number of samples (n) in each experimental condition is indicated in the corresponding figure legend. Outliers were assessed by the ROUT method,[<sup>57</sup>] thus any sample was excluded assuming a Q value of 1% in GraphPad Prism 9. Comparisons among experimental groups were performed by Student's t test or one-way analysis of variance (ANOVA) followed by Tukey's multiple comparisons post-hoc test using GraphPad Prism 9, as indicated.

## 3. Results and discussion

### 3.1. Design

The obtained library (Fig. 2), which contains five diversity points (R<sup>1</sup>, R<sup>2</sup>, R<sup>3</sup>, X, and the stereodisposition of R<sup>2</sup>), was designed to systematically explore the structural determinants governing the SCRA's bioactivity profile. We conceived a 64 members collection (Fig. 2) containing skeletal (indole and indazole), functional (esters and amides), alkylic (*iso*-propyl and *tert*-butyl) and stereochemical [(*S*) stereoisomers and (*R*) stereoisomers] diversity. The obtained library also features the four most frequent residues present at position 1 (*n*-pentyl, 5-fluoropentyl, 4-fluorobenzyl and cyclohexylmethyl) of the SCRA's heterocyclic cores (Fig. 2). To properly compile and evaluate SAR trends, the library contains 32 representative knon SCRA's. Notably, 32 of the 64 cannabinoid receptor agonists herein documented had not been previously reported (e.g., derivatives featuring the (*R*)

configuration within the pendant amino acid residue). Therefore, to our knowledge, this is the largest SCRA library ever published to date. For the sake of simplicity, and to allow a more direct appreciation of emerging SAR trends, the 64-membered collection was divided into four subsets, representing functional (esters or amides) and skeletal (indoles or indazoles) diversity (Scheme 1).

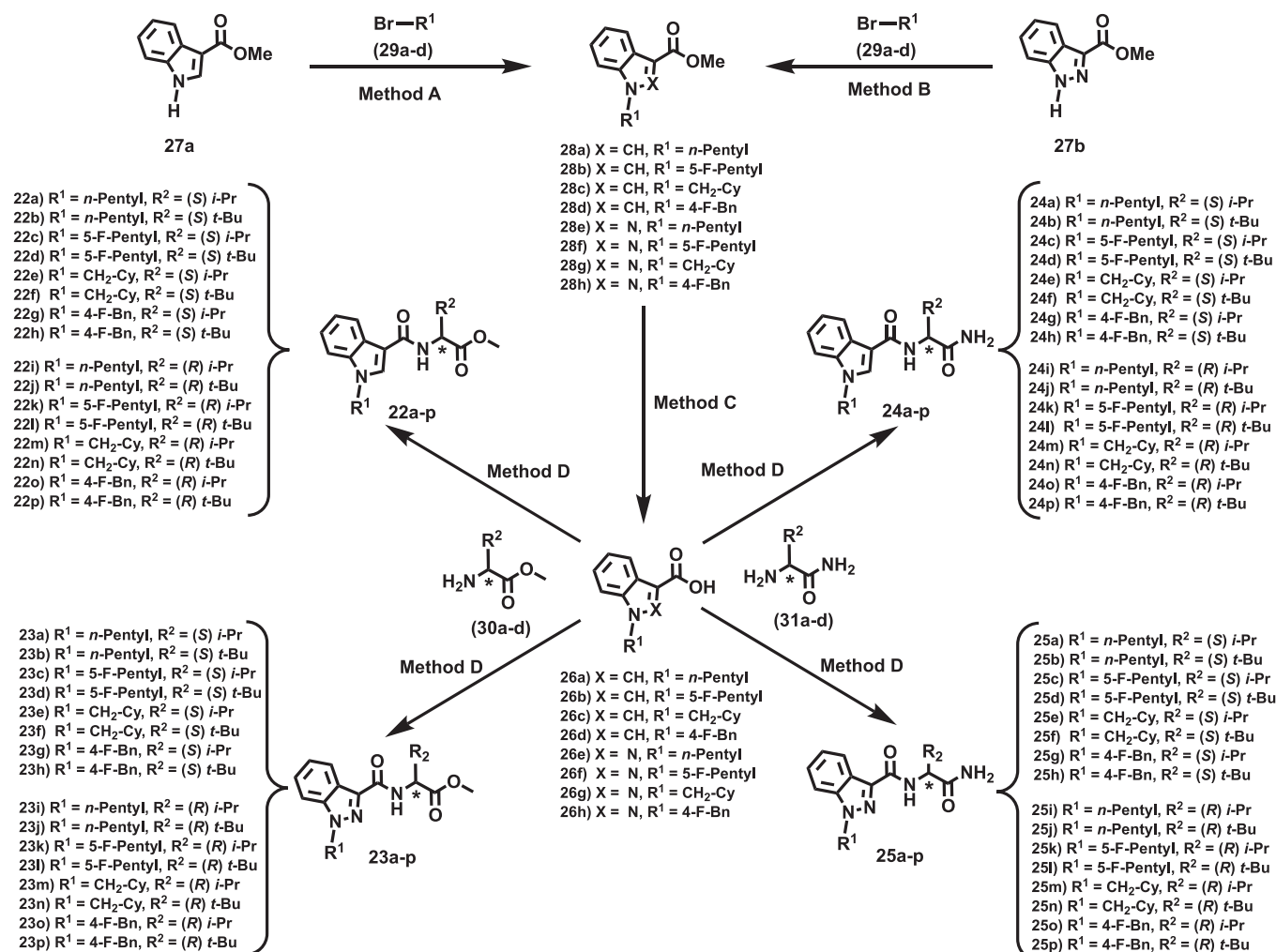
### 3.2. Chemistry

The targeted SCRA collection (Scheme 1, ligands 22a-p, 23a-p, 24a-p and 25a-p) was assembled following robust and well-established amide synthesis protocols (Scheme 1). The required carboxylic acids (26a-h) were prepared (Scheme 1, Method C), by saponification of the *N*-alkylated esters 28a-h. Esters 28 were obtained by alkylation of precursors 27 [methyl 3-indolecarboxylate (27a) and methyl 3-indazolecarboxylate (27b)] with four alkyl halides (29a-d) under basic conditions (Scheme 1, Methods A or B). The two regioisomers obtained during the alkylation of methyl 3-indazolecarboxylate (27b) were separated by chromatographic techniques (Scheme 1, Method B). The unambiguous identity of the major *N*<sup>1</sup>-alkylated compound (3:1 ratio) (28e-h) was confirmed by NMR experiments. Commercially available (Sigma Aldrich) enantiopure (ee ≥ 99%) amino acid derivatives [methyl glycinate derivatives (30a-d) and glycinate derivatives (31a-d)] of both the (*R*) and (*S*) series, bearing either *iso*-propyl or *tert*-butyl groups at R<sub>1</sub>, were used for the synthesis of targeted compounds (Scheme 1,

Method D). The amide coupling protocol (HATU) afforded the targeted derivatives (22a-p–25a-p) in moderate (47%) to excellent yields (96%) ensuring retention of the enantiomeric fidelity. [36].

All reactions were monitored by thin-layer chromatography (TLC) employing UV light, iodine, or a dissolution of phosphomolybdic acid for the compound's detection. After completion of the reaction, the solvent was evaporated to dryness and the isolated solid was purified by column chromatography on silica gel. A detailed description of the synthetic methods and the complete structural, spectroscopic, and analytical data for all compounds is provided in the experimental part and Supporting Information.

Although the carboxylic acids 26 are non-chiral, and racemization is mechanistically unlikely under the employed amide coupling conditions, [36,37] all members of the library were routinely controlled by analytical chiral HPLC to confirm that the stereocenter remained intact in the final compounds (see experimental part and Supporting Information). A selection of the HPLC traces obtained for representative enantiomeric pairs is presented in Fig. 3. Circular dichroism (CD) spectroscopy [38,39] is an orthogonal and versatile biophysical technique that provides valuable structural information [40,41] of proteins, peptides, small molecules, and functional macromolecules. As part of the characterization of herein described SCRA, it was envisioned that they contain the two structural requirements to interact with circularly polarized light used in CD spectroscopy: a chromophore (indole or indazole cores) and an enantiopure amino acid residue (chirality).



**Scheme 1.** Synthesis of the SCRA 22-25. Method A) NaH, DMF, rt, 24 h. Method B) NaH, DMF, rt, 24 h and then chromatographic separation to isolate the regioisomers. Method C) NaOH, dioxane, 120°C, 12 h. Method D) HATU, DIPEA, CH<sub>2</sub>Cl<sub>2</sub>, rt, 24 h.

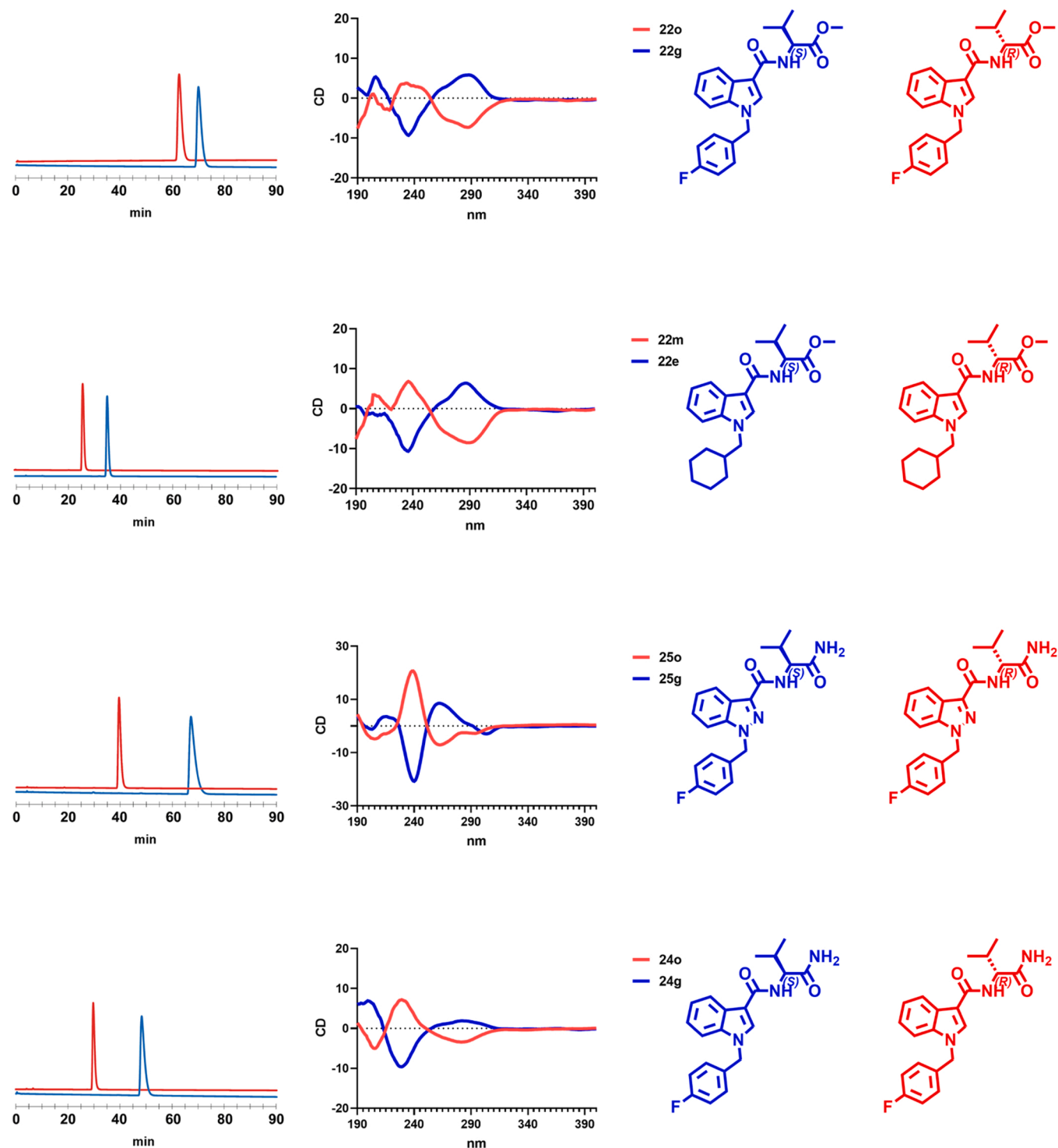


**Fig. 3.** HPLC traces of representative enantiopure esters and amides SCRA (left) and circular dichroism spectra of enantiomer pairs (right). At 240 nm the (S) enantiomer showed a negative Cotton effect (blue line), while the (R) stereoisomer gave a positive Cotton effect (red line).

Accordingly, it was decided to study the circular dichroism (CD) spectra of representative SCRA pairs, all experiments were performed employing enantiopure derivatives eliciting  $ee \geq 98\%$ . As observed (Fig. 3), irrespectively of the functional group within the amino acid residue (ester or amide), each single stereoisomer of the enantiomer pairs elicited symmetrical CD spectra, mirrored at the x-axis and with opposite sign. The absorbance of circularly polarized light by the chiral center in the SCRA gives rise to a characteristic CD signal at low wavelength (far-UV: 240 nm) that provides information about the

secondary structure (stereochemistry). On the other hand, the heterocyclic chromophore, despite being non-chiral, gives rise to CD signals in the near-UV (250–330 nm), because they are affected by the adjacent chiral environment. The characteristic CD signal around 240 nm allowed the unambiguous assignment of the absolute configuration of each enantiomer (Fig. 3). At this wavelength, the (S) enantiomer showed a negative Cotton effect (blue line), while the (R) stereoisomer gave a positive Cotton effect (red line). These additional experiments confirmed that all the obtained ligands contained a stereo-defined

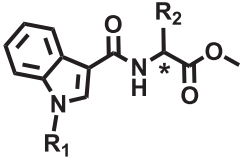
configuration and were pharmacologically evaluated as enantiopure compounds (ee >98%). In view of its robustness, performance and minimal sample preparation requirements, circular dichroism spectroscopy offers unique insights to rapidly assess the configuration of SCRA enantiopure samples.

### 3.3. Biological evaluation

One of the aims of this study was to address the limited availability of large SCRA collections and, consequently, the lack of homogeneous and reliable pharmacological data of these drugs of abuse. Thus, the cannabinimimetic profile of the 64 SCRAs was studied *in vitro* by evaluating its functional activity ( $EC_{50}$  and  $E_{max}$ ) and binding affinity ( $K_i$ ) for human  $CB_1$ Rs and  $CB_2$ Rs according to established experimental protocols. All the studied indole and indazole derivatives bind and activated

both  $CB_1$ R and  $CB_2$ R. The pharmacological data (Tables 1–4) are expressed as  $pEC_{50} \pm SEM$  or  $pK_i \pm SEM$  [and  $EC_{50}$  and  $K_i$  (nM)]. The data obtained for  $\Delta^9$ -THC, Surinabant, CP55,940 and GW405833, using described experimental protocols, were reported in tables for the sake of comparison. The *in vitro* affinity data was acquired via competitive radioligand binding assays using membrane preparations of human  $CB_1$ Rs and  $CB_2$ Rs transfected in CHO-CB1 C3 cells and HEK-293 T cells respectively and a well-characterized tritiated ligand ( $[^3H]$ CP55,940). As cannabinoid receptors are GPCRs coupled to the Gi protein, the functional activity of synthesized SCRAs at  $CB_1$ Rs and  $CB_2$ Rs was assessed by determining the decreases in cAMP levels induced by forskolin treatment. During functional experiments, the maximum effects of ligands 22–25 and  $\Delta^9$ -THC were normalized to a maximal efficacious concentration of CP 55,940. Data for each experiment were normalized to the change in fluorescence produced by a maximally effective

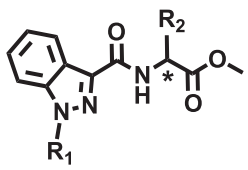
**Table 1**  
Structure, affinity, and functional data obtained for the indole esters 22a-p.



Compound	R <sup>1</sup>	R <sup>2</sup>	CB <sub>1</sub> R			CB <sub>2</sub> R			SI K <sub>i</sub> CB <sub>1</sub> R/ K <sub>i</sub> CB <sub>2</sub> R
			$pEC_{50} \pm SEM^a$ [EC <sub>50</sub> nM]	$E_{max} \pm SEM^b$ (% CP55940)	$pK_i \pm SEM^c$ [K <sub>i</sub> nM]	$pEC_{50} \pm SEM^a$ [EC <sub>50</sub> nM]	$E_{max} \pm SEM^b$ (% CP55940)	$pK_i \pm SEM^d$ [K <sub>i</sub> nM]	
22a (AMBICA) <sup>21</sup>	Pentyl	(S) <i>i</i> -Pr	7.27 ± 0.05 [53.7]	80%	7.58 ± 0.07 [26.6]	7.34 ± 0.05 [45.2]	77%	7.79 ± 0.09 [16.4]	1.62
22b (MDMB-PICA) <sup>21</sup>	Pentyl	(S) <i>t</i> -Bu	7.55 ± 0.03 [28.4]	74%	8.14 ± 0.05 [7.20]	8.94 ± 0.07 [1.14]	95%	8.54 ± 0.03 [2.90]	2.48
22c (5 F-AMBICA) <sup>21</sup>	5-F-Pentyl	(S) <i>i</i> -Pr	8.34 ± 0.06 [4.62]	134%	8.09 ± 0.08 [8.10]	8.98 ± 0.06 [1.05]	74%	8.38 ± 0.07 [4.23]	1.91
22d (5 F-MDMB-PICA) <sup>21</sup>	5-F-Pentyl	(S) <i>t</i> -Bu	9.15 ± 0.08 [0.70]	88%	8.59 ± 0.09 [2.61]	9.29 ± 0.07 [0.51]	103%	9.15 ± 0.05 [0.70]	3.73
22e (MMB-CHMICA) <sup>21</sup>	CH <sub>2</sub> -Cy	(S) <i>i</i> -Pr	7.74 ± 0.09 [18.1]	79%	7.98 ± 0.06 [10.5]	8.64 ± 0.08 [2.27]	68%	8.47 ± 0.07 [3.44]	3.05
22 f (MDBM-CHMICA) <sup>21</sup>	CH <sub>2</sub> -Cy	(S) <i>t</i> -Bu	8.82 ± 0.07 [1.50]	58%	10.05 ± 0.12 [0.09]	9.22 ± 0.09 [0.60]	61%	9.74 ± 0.08 [0.18]	0.50
22 g (MMB-FUBICA) <sup>21</sup>	4-F-Bn	(S) <i>i</i> -Pr	7.94 ± 0.05 [11.4]	88%	7.32 ± 0.03 [47.8]	7.32 ± 0.03 [48.2]	101%	7.70 ± 0.05 [20.0]	2.39
22 h (MDMB-FUBICA) <sup>21</sup>	4-F-Bn	(S) <i>t</i> -Bu	8.16 ± 0.07 [6.99]	75%	8.42 ± 0.08 [3.83]	8.67 ± 0.06 [2.12]	82%	8.95 ± 0.07 [1.12]	3.42
22i*	Pentyl	(R) <i>i</i> -Pr	7.14 ± 0.06 [72.3]	66%	6.20 ± 0.04 [632]	8.34 ± 0.07 [4.60]	94%	7.43 ± 0.09 [37.1]	17.1
22j*	Pentyl	(R) <i>t</i> -Bu	7.72 ± 0.08 [19.0]	126%	6.60 ± 0.02 [251]	7.24 ± 0.04 [57.0]	66%	6.69 ± 0.03 [110]	2.28
22k*	5-F-Pentyl	(R) <i>i</i> -Pr	8.16 ± 0.09 [6.92]	137%	7.22 ± 0.05 [60.2]	8.11 ± 0.07 [7.79]	104%	7.72 ± 0.05 [19.2]	3.14
22 l*	5-F-Pentyl	(R) <i>t</i> -Bu	7.83 ± 0.05 [14.9]	137%	6.89 ± 0.09 [127]	9.60 ± 0.06 [0.25]	126%	8.21 ± 0.04 [6.11]	20.8
22 m*	CH <sub>2</sub> -Cy	(R) <i>i</i> -Pr	7.86 ± 0.06 [13.9]	87%	7.12 ± 0.06 [76.4]	7.21 ± 0.08 [61.6]	107%	7.92 ± 0.08 [12.1]	6.31
22 n*	CH <sub>2</sub> -Cy	(R) <i>t</i> -Bu	7.75 ± 0.04 [17.6]	89%	6.82 ± 0.07 [151]	7.64 ± 0.03 [22.8]	64%	7.27 ± 0.03 [53.5]	2.82
22o*	4-F-Bn	(R) <i>i</i> -Pr	7.71 ± 0.06 [19.7]	109%	6.84 ± 0.04 [145]	8.30 ± 0.07 [5.01]	91%	8.10 ± 0.07 [8.21]	17.6
22p*	4-F-Bn	(R) <i>t</i> -Bu	7.88 ± 0.07 [13.2]	120%	6.75 ± 0.06 [179]	8.03 ± 0.06 [9.43]	49%	7.64 ± 0.05 [22.8]	7.85
$\Delta^9$ -THC	-	-	7.47 ± 0.16 [33.8]	51%	-	6.62 ± 0.25 [238]	21%	-	-
Surinabant	-	-	-	-	8.52 ± 0.08 [3.00]	-	-	6.39 ± 0.06 [400]	0.0075
GW405833	-	-	-	-	5.32 ± 0.05 [4772]	-	-	8.23 ± 0.07 [5.80]	822
CP55,940	-	-	-	-	8.99 ± 0.11 [1.01]	-	-	10.21 ± 0.32 [0.13]	7.76

<sup>a</sup>) Functional activity assessed in transfected HEK-293 T cells by determining cAMP levels after forskolin stimulation. <sup>b</sup>)  $E_{max}$  values were normalized to a maximal efficacious concentration of CP55,940. <sup>c</sup>) Displacement of specific [<sup>3</sup>H]CP 55,940 binding in membrane preparations of human  $CB_1$ Rs transfected in CHO-CB1 C3 cell line expressed as  $K_i$  in nM (n = 3) or percentage displacement of specific binding at a concentration of 1  $\mu$ M (n = 2). <sup>d</sup>) Displacement of specific [<sup>3</sup>H]CP 55,940 binding in membrane preparations of human  $CB_2$ Rs transfected in HEK-293 T cells expressed as  $K_i$  in nM (n = 3) or percentage displacement of specific binding at a concentration of 1  $\mu$ M (n = 2). \* These SCRAs have not been previously described.

**Table 2**  
Structure, affinity, and functional data obtained for the indazole esters **23a-p**.



Compound	R <sup>1</sup>	R <sup>2</sup>	CB <sub>1</sub> R			CB <sub>2</sub> R			SI K <sub>i</sub> CB <sub>1</sub> R/ K <sub>i</sub> CB <sub>2</sub> R
			pEC <sub>50</sub> ±SEM <sup>a)</sup> [EC <sub>50</sub> nM]	E <sub>max</sub> ±SEM <sup>b)</sup> (% CP55940)	pK <sub>i</sub> ±SEM <sup>c)</sup> [K <sub>i</sub> nM]	pEC <sub>50</sub> ±SEM <sup>a)</sup> [EC <sub>50</sub> nM]	E <sub>max</sub> ±SEM <sup>b)</sup> (% CP55940)	pK <sub>i</sub> ±SEM <sup>d)</sup> [K <sub>i</sub> nM]	
<b>23a</b> (AMB) <sup>21</sup>	Pentyl	(S) <i>i</i> -Pr	8.56 ± 0.08 [2.73]	72%	8.39 ± 0.09 [4.17]	8.79 ± 0.08 [1.61]	62%	8.89 ± 0.06 [1.30]	3.21
<b>23b</b> (MDMB-PINACA) <sup>21</sup>	Pentyl	(S) <i>t</i> -Bu	8.59 ± 0.07 [2.60]	66%	8.68 ± 0.09 [2.10]	9.89 ± 0.09 [0.13]	68%	9.70 ± 0.04 [0.26]	8.08
<b>23c</b> (5 F-AMB) <sup>21</sup>	5-F-Pentyl	(S) <i>i</i> -Pr	8.90 ± 0.04 [1.27]	90%	8.77 ± 0.06 [1.74]	9.24 ± 0.06 [0.58]	81%	9.30 ± 0.07 [0.52]	3.35
<b>23d</b> (5FMDBMPINACA) <sup>21</sup>	5-F-Pentyl	(S) <i>t</i> -Bu	9.24 ± 0.06 [0.58]	75%	9.10 ± 0.09 [0.80]	10.0 ± 0.09 [0.10]	88%	10.0 ± 0.08 [0.10]	8.00
<b>23e</b> (AMB-CHMINACA) <sup>21</sup>	CH <sub>2</sub> -Cy	(S) <i>i</i> -Pr	8.69 ± 0.07 [2.02]	104%	8.72 ± 0.05 [1.90]	8.05 ± 0.05 [8.82]	83%	9.30 ± 0.07 [0.51]	3.73
<b>23 f</b> (MDMB-CHMINACA) <sup>21</sup>	CH <sub>2</sub> -Cy	(S) <i>t</i> -Bu	9.12 ± 0.05 [0.76]	84%	9.00 ± 0.07 [1.08]	8.72 ± 0.06 [1.92]	76%	9.52 ± 0.08 [0.33]	3.27
<b>23 g</b> (AMB-FUBINACA) <sup>21</sup>	4-F-Bn	(S) <i>i</i> -Pr	8.64 ± 0.09 [2.29]	115%	8.14 ± 0.03 [3.90]	9.92 ± 0.08 [0.12]	80%	9.22 ± 0.05 [0.62]	6.29
<b>23 h</b> (MDMBFUBINACA) <sup>21</sup>	4-F-Bn	(S) <i>t</i> -Bu	9.04 ± 0.07 [0.92]	81%	9.10 ± 0.02 [0.83]	9.77 ± 0.06 [0.17]	82%	9.52 ± 0.07 [0.30]	2.77
<b>23i*</b>	Pentyl	(R) <i>i</i> -Pr	8.04 ± 0.06 [9.02]	58%	7.04 ± 0.04 [91.6]	8.59 ± 0.09 [2.6]	98%	8.18 ± 0.06 [6.61]	13.8
<b>23j*</b>	Pentyl	(R) <i>t</i> -Bu	7.67 ± 0.04 [21.6]	100%	6.36 ± 0.07 [435]	8.38 ± 0.07 [4.2]	104%	7.85 ± 0.04 [14.7]	29.6
<b>23k*</b>	5-F-Pentyl	(R) <i>i</i> -Pr	8.10 ± 0.06 [7.91]	67%	7.63 ± 0.08 [23.5]	8.94 ± 0.05 [1.14]	70%	8.59 ± 0.09 [2.60]	9.04
<b>23 l*</b>	5-F-Pentyl	(R) <i>t</i> -Bu	7.29 ± 0.03 [51.3]	66%	7.09 ± 0.08 [81.1]	9.27 ± 0.07 [0.54]	87%	7.86 ± 0.05 [13.3]	6.10
<b>23 m*</b>	CH <sub>2</sub> -Cy	(R) <i>i</i> -Pr	8.18 ± 0.05 [6.59]	130%	7.61 ± 0.05 [24.4]	8.66 ± 0.06 [2.17]	92%	8.85 ± 0.07 [1.40]	17.4
<b>23 n*</b>	CH <sub>2</sub> -Cy	(R) <i>t</i> -Bu	8.28 ± 0.07 [5.26]	138%	7.42 ± 0.03 [38.4]	8.75 ± 0.06 [1.79]	106%	8.10 ± 0.06 [8.05]	4.77
<b>23o*</b>	4-F-Bn	(R) <i>i</i> -Pr	8.28 ± 0.04 [5.22]	134%	7.56 ± 0.07 [29.7]	8.83 ± 0.08 [1.49]	118%	9.00 ± 0.07 [1.20]	24.7
<b>23p*</b>	4-F-Bn	(R) <i>t</i> -Bu	8.36 ± 0.09 [4.35]	152%	7.16 ± 0.03 [68.4]	7.88 ± 0.04 [13.2]	91%	8.17 ± 0.09 [6.70]	10.2
Δ <sup>9</sup> -THC	-	-	7.47 ± 0.16 [33.8]	51%	-	6.62 ± 0.25 [238]	21%	-	-
Surinabant	-	-	-	-	8.52 ± 0.08 [3.00]	-	-	6.39 ± 0.06 [400]	0.0075
GW405833	-	-	-	-	5.32 ± 0.05 [4772]	-	-	8.23 ± 0.07 [5.80]	822
CP55,940	-	-	-	-	8.99 ± 0.11 [1.01]	-	-	10.21 ± 0.32 [0.13]	7.76

<sup>a)</sup> Functional activity assessed in transfected HEK-293 T cells by determining cAMP levels after forskolin stimulation. <sup>b)</sup> E<sub>max</sub> values were normalized to a maximal efficacious concentration of CP55,940. <sup>c)</sup> Displacement of specific [<sup>3</sup>H]CP 55,940 binding in membrane preparations of human CB<sub>1</sub>R transfected in CHO-CB1 C3 cell line expressed as K<sub>i</sub> in nM (n = 3) or percentage displacement of specific binding at a concentration of 1 μM (n = 2). <sup>d)</sup> Displacement of specific [<sup>3</sup>H]CP 55,940 binding in membrane preparations of human CB<sub>2</sub>R transfected in HEK-293 T cells expressed as K<sub>i</sub> in nM (n = 3) or percentage displacement of specific binding at a concentration of 1 μM (n = 2). \* These SCRA have not been previously described.

concentration of CP 55,940.

Representative dose-response curves obtained for selected ligands during the functional studies and binding affinity determinations at CB<sub>1</sub>R and CB<sub>2</sub>R, are presented in Fig. 4. A detailed description of the protocols is reported in the experimental part. The dose-response curves obtained for all the ligands documented here are given in the Supporting Information.

The pharmacological data obtained for the 64-membered collection are presented in Tables 1–4, each one containing 16 derivatives [the first 8 bearing the (S) configuration at the pendant amino acid residue and the other 8 the (R) configuration]. Tables 1 and 2 present the pharmacological data of esters (indoles and indazoles respectively) while Tables 3 and 4 report the data obtained for amides (indole and indazoles respectively). Novel compounds are indicated with an asterisk (Tables 1–4) and already described SCRA with their common acronym

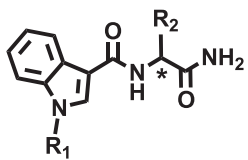
in the illicit drug market (Tables 1–4). The original articles describing the known compounds are listed in tables. [7,21,24] To facilitate the identification of the most salient features of the structure-selectivity relationship throughout the series, the selectivity index (SI), calculated using the affinity data (K<sub>i</sub> CB<sub>2</sub>R/K<sub>i</sub> CB<sub>1</sub>R), was also reported in Tables 1–4.

### 3.4. Structure-Activity Relationship analysis

The binding affinities (pK<sub>i</sub>), potencies (pEC<sub>50</sub>) and efficacies (E<sub>max</sub>) obtained during the pharmacological evaluation of the library (22ap–25ap) at CB<sub>1</sub>R and CB<sub>2</sub>R are presented in Table 1–4. The affinity and functional data herein determined for known SCRA (22–25a-h) are in the same range as reported (see Table 1S, supporting information). [5,7,8,10,20] For comparative purposes the phytocannabinoid



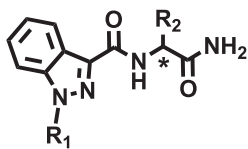
**Table 3**  
Structure, affinity, and functional data obtained for the indole amides **24a-p**.



Compound	R <sup>1</sup>	R <sup>2</sup>	CB <sub>1</sub> R			CB <sub>2</sub> R			SI K <sub>i</sub> CB <sub>1</sub> R/ K <sub>i</sub> CB <sub>2</sub> R
			pEC <sub>50</sub> ±SEM <sup>a)</sup> [EC <sub>50</sub> nM]	E <sub>max</sub> ±SEM <sup>b)</sup> (% CP55940)	pK <sub>i</sub> ±SEM <sup>c)</sup> [K <sub>i</sub> nM]	pEC <sub>50</sub> ±SEM <sup>a)</sup> [EC <sub>50</sub> nM]	E <sub>max</sub> ±SEM <sup>b)</sup> (% CP55940)	pK <sub>i</sub> ±SEM <sup>d)</sup> [K <sub>i</sub> nM]	
<b>24a</b> (AB-PICA) <sup>24</sup>	Pentyl	(S) <i>i</i> -Pr	6.92 ± 0.02 [1.20]	85%	7.76 ± 0.03 [17.5]	8.36 ± 0.07 [4.32]	120%	7.95 ± 0.04 [11.2]	1.56
<b>24b</b> (AD-BICA) <sup>24</sup>	Pentyl	(S) <i>t</i> -Bu	8.79 ± 0.07 [1.64]	76%	9.10 ± 0.08 [0.80]	9.00 ± 0.09 [1.00]	105%	9.30 ± 0.09 [0.52]	1.54
<b>24c</b> (5 F-AB-PICA) <sup>24</sup>	5-F- Pentyl	(S) <i>i</i> -Pr	8.31 ± 0.07 [4.95]	109%	7.83 ± 0.07 [14.8]	8.67 ± 0.09 [2.15]	123%	8.07 ± 0.05 [8.60]	1.72
<b>24d</b> (5 F-AD-BICA) <sup>24</sup>	5-F- Pentyl	(S) <i>t</i> -Bu	7.88 ± 0.03 [13.1]	109%	9.05 ± 0.09 [0.91]	9.62 ± 0.05 [0.24]	122%	9.15 ± 0.09 [0.74]	1.23
<b>24e</b> (AB-CHMICA) <sup>7</sup>	CH <sub>2</sub> -Cy	(S) <i>i</i> -Pr	9.60 ± 0.07 [0.25]	95%	8.62 ± 0.09 [2.43]	8.70 ± 0.07 [1.98]	86%	7.45 ± 0.04 [35.3]	0.07
<b>24 f</b> (ADB- CHMICA) <sup>7</sup>	CH <sub>2</sub> -Cy	(S) <i>t</i> -Bu	6.66 ± 0.05 [221]	70%	8.96 ± 0.07 [1.10]	8.09 ± 0.03 [8.20]	73%	9.12 ± 0.06 [0.76]	1.45
<b>24 g</b> (AB-FUBICA) <sup>24</sup>	4-F-Bn	(S) <i>i</i> -Pr	7.94 ± 0.04 [11.5]	89%	7.45 ± 0.04 [35.2]	8.04 ± 0.07 [9.15]	86%	6.22 ± 0.06 [83.2]	0.42
<b>24 h</b> (ADB- FUBICA) <sup>24</sup>	4-F-Bn	(S) <i>t</i> -Bu	7.19 ± 0.06 [64.1]	69%	7.27 ± 0.04 [53.8]	8.95 ± 0.09 [1.11]	77%	8.29 ± 0.07 [5.15]	10.4
<b>24i*</b>	Pentyl	(R) <i>i</i> -Pr	8.30 ± 0.09 [4.96]	95%	6.17 ± 0.03 [672]	7.52 ± 0.04 [29.9]	117%	6.48 ± 0.05 [328]	2.05
<b>24j*</b>	Pentyl	(R) <i>t</i> -Bu	8.60 ± 0.08 [2.54]	92%	7.19 ± 0.07 [65]	8.88 ± 0.09 [1.32]	102%	7.69 ± 0.04 [20.3]	3.20
<b>24k*</b>	5-F- Pentyl	(R) <i>i</i> -Pr	6.59 ± 0.04 [258]	72%	6.14 ± 0.08 [720]	6.15 ± 0.08 [703]	42%	6.37 ± 0.07 [425]	1.69
<b>24 l*</b>	5-F- Pentyl	(R) <i>t</i> -Bu	7.20 ± 0.06 [62.7]	59%	7.04 ± 0.06 [90.6]	8.88 ± 0.07 [1.33]	77%	7.82 ± 0.09 [15.1]	6.00
<b>24 m*</b>	CH <sub>2</sub> -Cy	(R) <i>i</i> -Pr	7.08 ± 0.04 [82.5]	47%	6.51 ± 0.03 [311]	6.65 ± 0.05 [225]	48%	6.96 ± 0.05 [109]	2.85
<b>24 n*</b>	CH <sub>2</sub> -Cy	(R) <i>t</i> -Bu	8.31 ± 0.07 [4.90]	81%	7.18 ± 0.05 [66.1]	8.60 ± 0.05 [2.49]	54%	7.66 ± 0.06 [21.8]	3.03
<b>24o*</b>	4-F-Bn	(R) <i>i</i> -Pr	7.41 ± 0.03 [39.1]	85%	6.00 ± 0.07 [588]	8.08 ± 0.08 [8.38]	82%	6.78 ± 0.08 [167]	3.52
<b>24p*</b>	4 F-Bn	(R) <i>t</i> -Bu	7.83 ± 0.04 [14.8]	127%	7.14 ± 0.06 [72.8]	8.49 ± 0.07 [3.24]	79%	7.63 ± 0.03 [23.3]	3.12
<b>Δ<sup>9</sup>-THC</b>	-	-	7.47 ± 0.16 [33.8]	51%	-	6.62 ± 0.25 [238]	21%	-	-
<b>Surinabant</b>	-	-	-	-	8.52 ± 0.08 [3.00]	-	-	6.39 ± 0.06 [400]	0.0075
<b>GW405833</b>	-	-	-	-	5.32 ± 0.05 [4772]	-	-	8.23 ± 0.07 [5.80]	822
<b>CP55,940</b>	-	-	-	-	8.99 ± 0.11 [1.01]	-	-	10.21 ± 0.32 [0.13]	7.76

<sup>a)</sup> Functional activity assessed in transfected HEK-293 T cells by determining cAMP levels after forskolin stimulation. <sup>b)</sup> E<sub>max</sub> values were normalized to a maximal efficacious concentration of CP55,940. <sup>c)</sup> Displacement of specific [<sup>3</sup>H]CP 55,940 binding in membrane preparations of human CB<sub>1</sub>Rs transfected in CHO-CB1 C3 cell line expressed as K<sub>i</sub> in nM (n = 3) or percentage displacement of specific binding at a concentration of 1 μM (n = 2). <sup>d)</sup> Displacement of specific [<sup>3</sup>H]CP 55,940 binding in membrane preparations of human CB<sub>2</sub>Rs transfected in HEK-293 T cells expressed as K<sub>i</sub> in nM (n = 3) or percentage displacement of specific binding at a concentration of 1 μM (n = 2). \* These SCRA have not been previously described.

**Table 4**  
Structure, affinity, and functional data obtained for the indazole amides **25a-p**.



Compound	R <sup>1</sup>	R <sup>2</sup>	CB <sub>1</sub> R			CB <sub>2</sub> R			SI K <sub>i</sub> CB <sub>1</sub> R/ K <sub>i</sub> CB <sub>2</sub> R
			pEC <sub>50</sub> ±SEM <sup>a)</sup> [EC <sub>50</sub> nM]	E <sub>max</sub> ±SEM <sup>b)</sup> (% CP55940)	pK <sub>i</sub> ±SEM <sup>c)</sup> [K <sub>i</sub> nM]	pEC <sub>50</sub> ±SEM <sup>a)</sup> [EC <sub>50</sub> nM]	E <sub>max</sub> ±SEM <sup>b)</sup> (% CP55940)	pK <sub>i</sub> ±SEM <sup>d)</sup> [K <sub>i</sub> nM]	
<b>25a</b> (AB-PINACA) <sup>24</sup>	Pentyl	(S) <i>i</i> -Pr	8.83 ± 0.07 [1.49]	94%	8.96 ± 0.08 [1.16]	9.68 ± 0.09 [0.21]	128%	9.05 ± 0.08 [0.94]	1.23
<b>25b</b> (ADB-PINACA) <sup>24</sup>	Pentyl	(S) <i>t</i> -Bu	11.0 ± 0.09 [0.01]	138%	9.40 ± 0.08 [0.40]	9.89 ± 0.08 [0.13]	129%	9.52 ± 0.08 [0.30]	1.33
<b>25c</b> (5 F-AB-PINACA) <sup>24</sup>	5-F-Pentyl	(S) <i>i</i> -Pr	8.87 ± 0.09 [1.36]	164%	7.75 ± 0.07 [17.9]	9.17 ± 0.06 [0.67]	127%	7.84 ± 0.05 [14.3]	1.25
<b>25d</b> (5 F-ADB-PINACA) <sup>24</sup>	5-F-Pentyl	(S) <i>t</i> -Bu	8.91 ± 0.08 [1.22]	134%	8.57 ± 0.05 [2.73]	9.44 ± 0.07 [0.36]	135%	9.52 ± 0.03 [0.31]	8.81
<b>25e</b> (AB-CHMINACA) <sup>7</sup>	CH <sub>2</sub> -Cy	(S) <i>i</i> -Pr	8.89 ± 0.06 [1.04]	78%	9.05 ± 0.09 [0.90]	8.12 ± 0.08 [7.67]	63%	8.96 ± 0.06 [1.10]	0.82
<b>25 f</b> (ABD-CHMINACA) <sup>7</sup>	CH <sub>2</sub> -Cy	(S) <i>t</i> -Bu	7.34 ± 0.04 [46.2]	80%	9.05 ± 0.09 [0.98]	8.46 ± 0.04 [3.49]	53%	9.22 ± 0.09 [0.60]	1.63
<b>25 g</b> (AB-FUBINACA) <sup>24</sup>	4-F-Bn	(S) <i>i</i> -Pr	8.41 ± 0.08 [3.86]	95%	8.64 ± 0.06 [2.31]	8.24 ± 0.06 [5.77]	86%	8.96 ± 0.08 [1.17]	1.97
<b>25 h</b> (ADB-FUBINACA) <sup>24</sup>	4-F-Bn	(S) <i>t</i> -Bu	7.67 ± 0.03 [21.3]	104%	9.10 ± 0.04 [0.83]	8.40 ± 0.08 [3.96]	84%	10.0 ± 0.07 [0.14]	5.93
<b>25i</b> *	Pentyl	(R) <i>i</i> -Pr	7.99 ± 0.02 [10.3]	137%	6.98 ± 0.06 [105]	8.95 ± 0.06 [1.12]	113%	7.43 ± 0.05 [37.3]	2.82
<b>25j</b> *	Pentyl	(R) <i>t</i> -Bu	8.05 ± 0.03 [8.82]	131%	7.51 ± 0.05 [30.8]	8.71 ± 0.03 [1.97]	109%	7.92 ± 0.03 [12.1]	2.55
<b>25k</b> *	5-F-Pentyl	(R) <i>i</i> -Pr	7.32 ± 0.06 [48.2]	97%	6.79 ± 0.07 [160]	7.43 ± 0.07 [36.9]	65%	6.87 ± 0.02 [133]	1.20
<b>25 l</b> *	5-F-Pentyl	(R) <i>t</i> -Bu	7.02 ± 0.04 [95.7]	96%	6.28 ± 0.04 [520]	7.71 ± 0.06 [19.4]	54%	6.66 ± 0.08 [221]	2.35
<b>25 m</b> *	CH <sub>2</sub> -Cy	(R) <i>i</i> -Pr	7.75 ± 0.03 [17.7]	100%	7.75 ± 0.08 [17.9]	7.57 ± 0.04 [26.9]	43%	7.61 ± 0.07 [24.5]	0.73
<b>25 n</b> *	CH <sub>2</sub> -Cy	(R) <i>t</i> -Bu	8.60 ± 0.05 [2.50]	130%	7.71 ± 0.07 [19.4]	7.24 ± 0.06 [57.2]	52%	7.77 ± 0.05 [17.2]	1.13
<b>25o</b> *	4-F-Bn	(R) <i>i</i> -Pr	8.65 ± 0.05 [2.25]	126%	6.85 ± 0.06 [139]	5.89 ± 0.03 [1301]	93%	7.07 ± 0.09 [84.3]	1.65
<b>25p</b> *	4-F-Bn	(R) <i>t</i> -Bu	7.70 ± 0.07 [19.8]	106%	7.85 ± 0.03 [26.2]	7.44 ± 0.07 [36.4]	89%	7.95 ± 0.06 [11.2]	2.34
$\Delta^9$ -THC	-	-	7.47 ± 0.16 [33.8]	51%	-	6.62 ± 0.25 [238]	21%	-	-
Surinabant	-	-	-	-	8.52 ± 0.08 [3.00]	-	-	6.39 ± 0.06 [400]	0.0075
GW405833	-	-	-	-	5.32 ± 0.05 [4772]	-	-	8.23 ± 0.07 [5.80]	822
CP55,940	-	-	-	-	8.99 ± 0.11 [1.01]	-	-	10.21 ± 0.32 [0.13]	7.76

<sup>a)</sup> Functional activity assessed in transfected HEK-293 T cells by determining cAMP levels after forskolin stimulation. <sup>b)</sup> E<sub>max</sub> values were normalized to a maximal efficacious concentration of CP55,940. <sup>c)</sup> Displacement of specific [<sup>3</sup>H]CP 55,940 binding in membrane preparations of human CB<sub>1</sub>Rs transfected in CHO-CB<sub>1</sub> C3 cell line expressed as K<sub>i</sub> in nM (n = 3) or percentage displacement of specific binding at a concentration of 1 μM (n = 2). <sup>d)</sup> Displacement of specific [<sup>3</sup>H]CP 55,940 binding in membrane preparations of human CB<sub>2</sub>Rs transfected in HEK-293 T cells expressed as K<sub>i</sub> in nM (n = 3) or percentage displacement of specific binding at a concentration of 1 μM (n = 2). \* These SCRA have not been previously described.

$\Delta^9$ -THC and three synthetic CBR ligands (surinabant, GW405833 and CP55,940) were evaluated with the same experimental protocols and their functional ( $\Delta^9$ -THC) or affinity (surinabant, GW405833 and CP55,940) data were also included in Table 1–4. The functional data obtained unequivocally confirm that derivatives **22–25** activate both CB<sub>1</sub>Rs and CB<sub>2</sub>Rs. In contrast with  $\Delta^9$ -THC (a partial agonist with moderate activity at both receptors), all members of the library (**22ap–25ap**) exhibited excellent activity and greater potency than  $\Delta^9$ -THC at both CB<sub>1</sub>Rs and CB<sub>2</sub>Rs. Comparison of the affinity (pK<sub>i</sub>) and functional (pEC<sub>50</sub>) values obtained for the members of the library (Tables 1–4) with published data reveals that there are no significant differences (supporting information Table 1S). As a general trend, the functional data (especially in CB<sub>2</sub>R) are slightly higher than reported. It is however well documented [42] that functional data (EC<sub>50</sub>) and efficacy (E<sub>max</sub>) are highly dependent on the expression level of the

receptors or “receptor reserve”, while K<sub>i</sub> values obtained in binding studies are largely independent on the employed cellular background. For these reasons, affinity data (pK<sub>i</sub>) will be used for subtype selectivity analysis and to establish the most of salient SAR and SSR features within the collection.

As stated in the introduction, the herein obtained comprehensive library is intended to be used (in a collaborative manner) with academics and law enforcement to address and control the threat to human health of this family of NPS. In addition, SAR observations from this large subset inspired our ongoing research project aimed at developing CB<sub>2</sub>R agonists as candidates for autoimmune and inflammatory diseases.

A first inspection of the data included in Tables 1–4 reveals that most of the ligands studied show a very consistent profile, generally behaving as highly potent, non-selective, full agonists at both receptors, regardless of their functional (ester or amide), skeletal (indole or indazole),

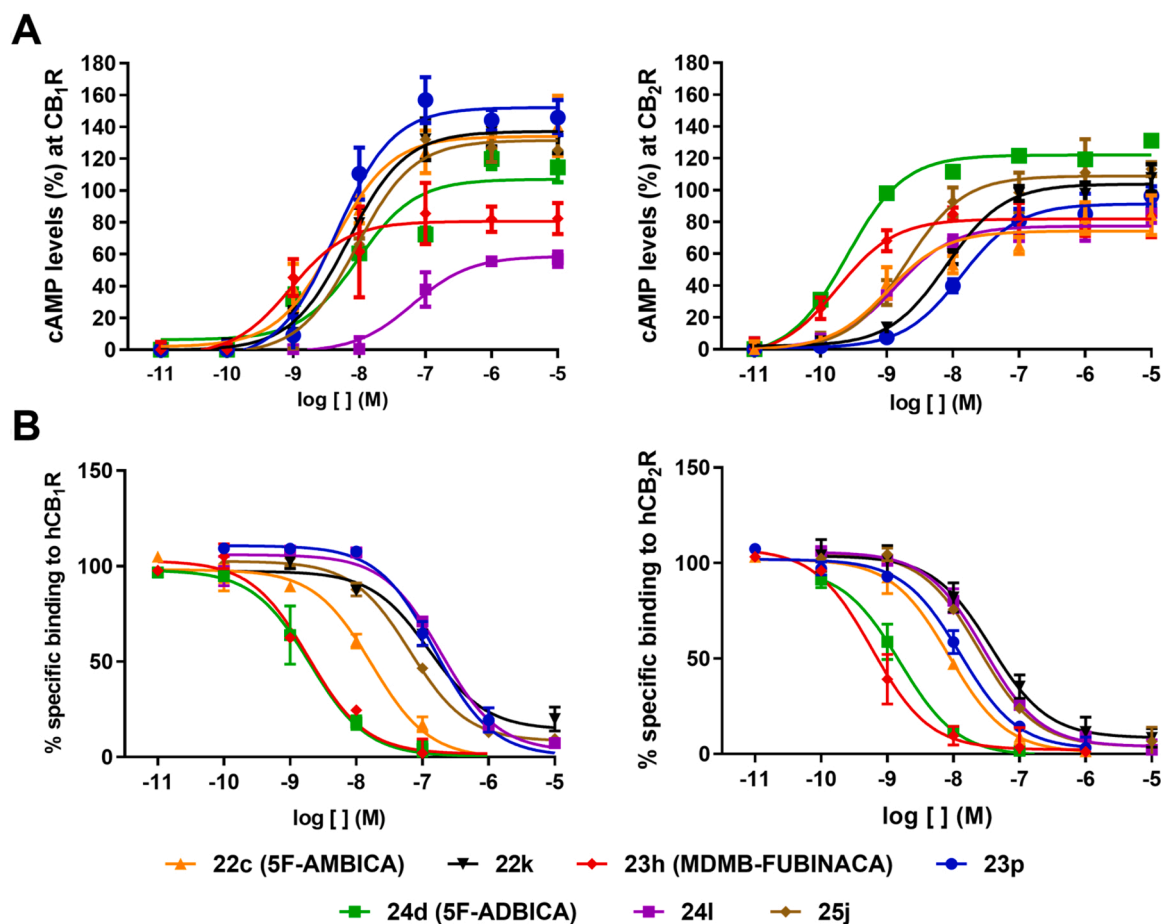


Fig. 4. Representative dose-response curves obtained for selected ligands at CB<sub>1</sub>R and CB<sub>2</sub>R during functional (4 A) and binding studies (4B).

stereochemical (*S* or *R*) or alkyl (*R*<sup>1</sup> and *R*<sup>2</sup>) diversity. According to their in vitro cannabinomimetic profiles (Tables 1–4), of the novel 32 ligands herein reported [bearing the (*R*) configuration at the pendant amino acid chain], fourteen derivatives (e.g., ligands 22k, 22p, 23 m, 23 n, 23o, 23p, 24i, 24j, 24 n, 24p, 25i, 25j, 25 n, 25o) present the prototypical profile of SCRA (e.g., low nanomolar affinity and activity, generally combined with high efficacy) and therefore could be (or may currently be) used as illegal psychoactive substances (prophetic SCRA).

As observed (Fig. 5), functional data reveal that most of these prophetic SCRA are significantly more efficacious at the CB<sub>1</sub>R. Thus, these derivatives (Fig. 5) deserve attention/monitoring by regulatory authorities (e.g., European Monitoring Centre for Drugs and Drug Addiction (EMCDDA) and United Nations Office on Drugs and Crime (UNODC)) and the scientific community. Further studies are now in progress in our laboratories to complete the pharmacological, functional selectivity and toxicological characterization of these 14 novel derivatives and commonly abused SCRA. However, it is worth noting that recent legislation in some countries has shifted towards a more comprehensive approach to controlling the emergence of SCRA, thus one might expect typical structure would be less likely to emerge on the recreational drug market.

For the sake of clarity, the discussion of the structure-activity relationship (SAR) trends, and to a lesser extent of the structure-selectivity relationship (SSR), is made here in an integrated fashion, according to the structural classifications reported in Scheme 1 and Tables 1–4. The affinity data was employed to rapidly evaluate trends and compare profiles, and then the analysis complemented with the functional information. For a more immediate and efficient analysis of the variation of both affinity and selectivity, the binding data (*p*K<sub>i</sub>) are presented graphically as a plot of *p*K<sub>i</sub> CB<sub>1</sub>R (*Y* axis) versus *p*K<sub>i</sub> CB<sub>2</sub>R (*X* axis) using

the same scale and range for both axes (square plot) in Figs. 6–8. On the diagonal of this plot (*Y* = *X*) compounds with equal affinities at both receptors will be found, whereas CB<sub>1</sub>R or CB<sub>2</sub>R selective compounds will be seen below or above the diagonal, respectively. The distance of their *p*K<sub>i</sub> values from the diagonal is a direct measure of their degree of selectivity.

We first focused on the analysis of the two main functional series herein described (esters and amides). *p*K<sub>i</sub> values ranging from 6.20 to 10.05 and from 6.22 to 10.00 were measured for the CB<sub>1</sub>R and the CB<sub>2</sub>R respectively. Their relationship and distribution are represented as a plot of *p*K<sub>i</sub> CB<sub>1</sub>R vs *p*K<sub>i</sub> CB<sub>2</sub>R in Fig. 6 for esters (6 A) and amides (6B). The skeletal diversity (scaffold) in each subset is represented in colors (red: indoles, blue: indazoles). A simple visual inspection of the plots (Fig. 6) for both functional series (plot A: esters, plot B: amides) revealed that CB<sub>1</sub>R and CB<sub>2</sub>R binding affinities are highly correlated [non-selective (dual) CB<sub>1</sub>R - CB<sub>2</sub>R profile]. In the ester series most of the examined ligands are slightly more affine toward the CB<sub>2</sub>R subtype [particularly indazole-based derivatives (blue circles)]. The exception to this trend is the indole derivative 22 f, lying slightly above the diagonal of the plot, its dual profile is observed also comparing its functional data. Seven ester derivatives (22i, 22 l, 22o, 23i, 23j, 23 m, 23o) fall below the second dashed diagonal line on the graph (Fig. 6), showing some selectivity (13–29 fold) towards CB<sub>2</sub>R. Analysis of the functional data (EC<sub>50</sub>) obtained for these ligands confirmed the incipient selectivity toward CB<sub>2</sub>R. A superior correlation among CB<sub>1</sub>R and CB<sub>2</sub>R binding affinities [evidencing highly dual CB<sub>1</sub>R - CB<sub>2</sub>R profile] is appreciated within the amide subset (Fig. 6, plot B), with most of the amides standing near the diagonal of the square plot. Anyhow, most of them are somewhat more affine towards the CB<sub>2</sub>R subtype. Two amide derivatives [one indazole (25d) and one indole (24 h)] elicit an incipient

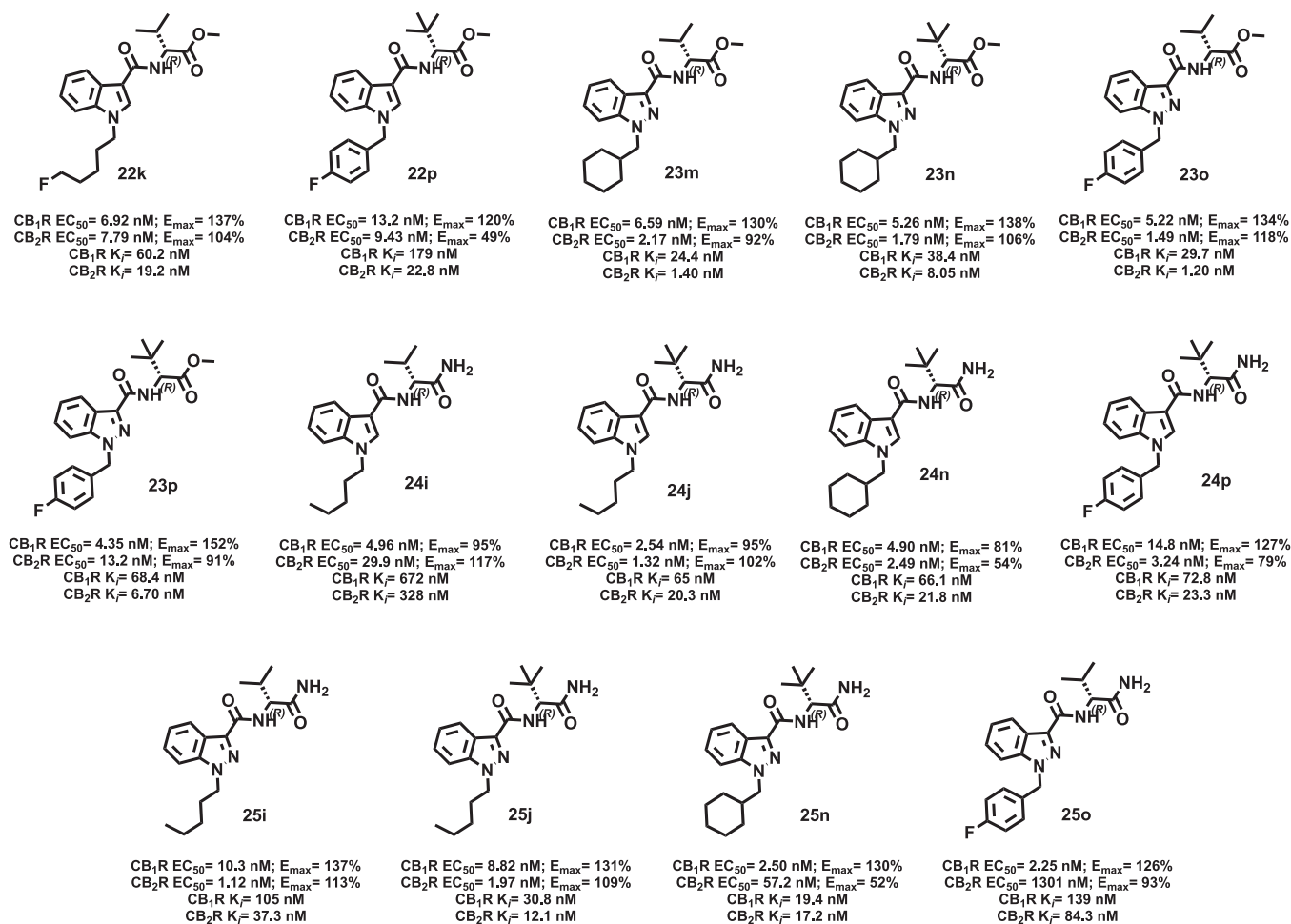


Fig. 5. Structure and cannabinomimetic data of the 14 previously unexplored (R) derivatives that show a pharmacological profile like that of commonly abused SCRAAs.

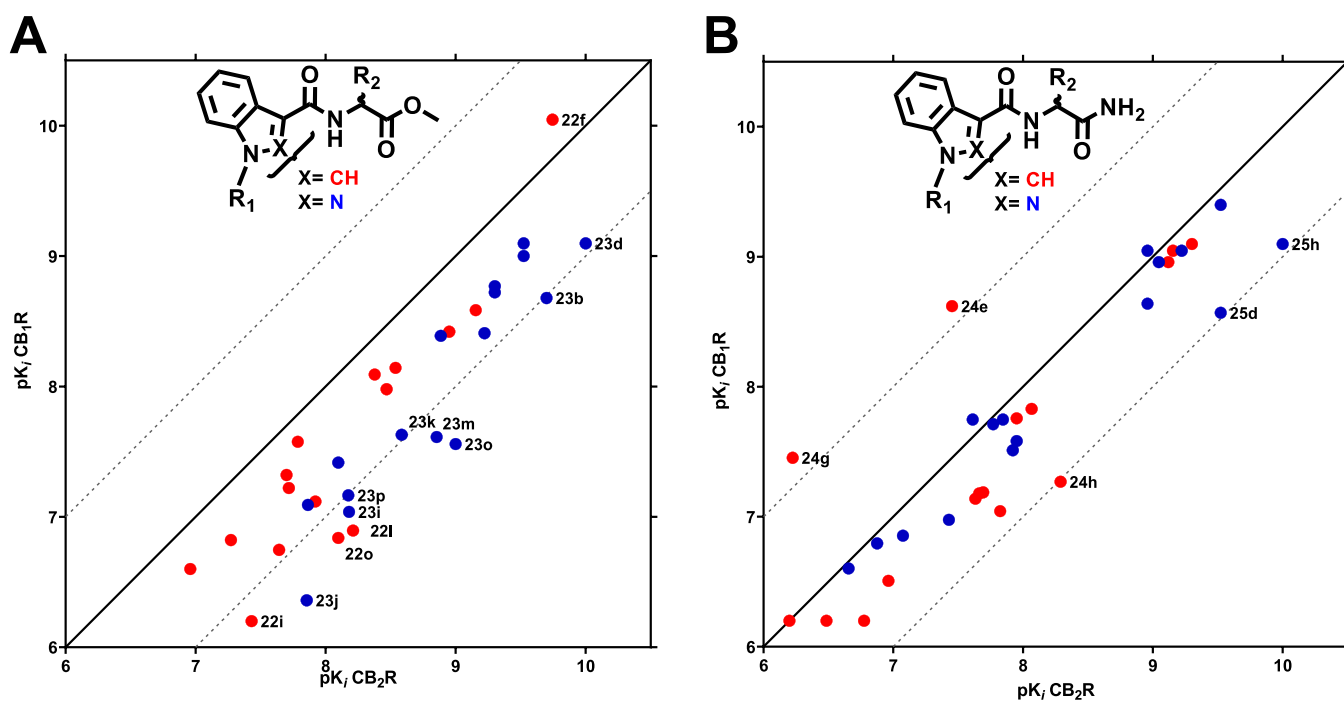


Fig. 6. Affinity-selectivity plot for 32 esters (6 A) and 32 amides (6B) obtained.

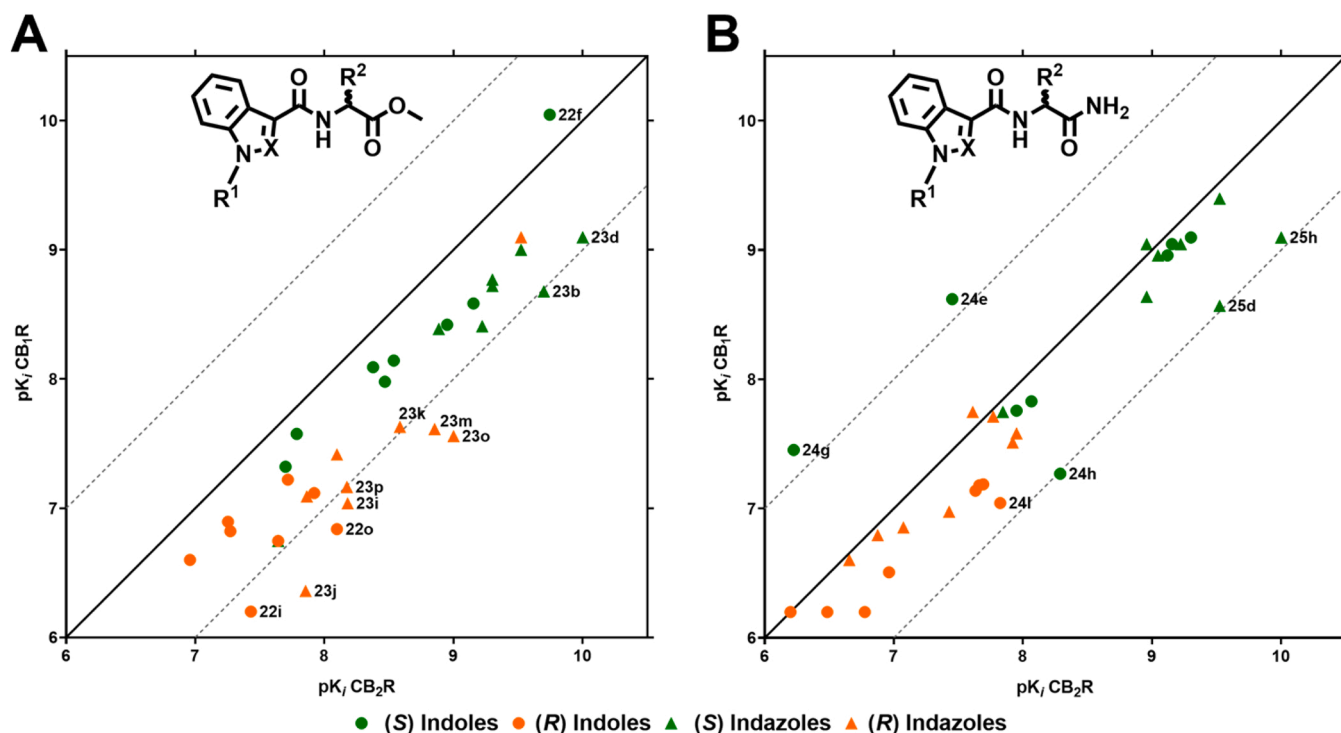


Fig. 7. Influence of the stereochemistry in the cannabinomimetic profile. Affinity-selectivity plots for (S) and (R) in the esters (7 A) and 32 amides (7B).

selectivity ( $\approx 10$ -fold) towards CB<sub>2</sub>R (Fig. 6B). In clear contrast to this trend, ligands **24 g** and **24 e** exhibit some CB<sub>1</sub>R selectivity. The incipient selectivities observed for **25d**, **24 h**, **24 g** and **24 e** are generally corroborated when comparing their functional data.

Taken together, the affinity data suggest that the functional diversity (ester or amide) is a more important contributor than the skeletal diversity (heterocyclic core) in defining the potency and selectivity profile in this series. The large set of ligands and the comprehensive pharmacological data documented here (Fig. 6) reveal new features of the SCRA's behavior, while providing additional validation to the reported observations. [43].

Fig. 7 was designed to gain insight into the contribution of the stereodisposition (R or S) of the R<sup>2</sup> group in the cannabinomimetic profile (potency and selectivity) of the ligands herein documented. For the analysis, the collection was divided into two subsets, esters (7 A) and amides (7B), with the binding affinity presented graphically as a plot of pK<sub>i</sub> CB<sub>1</sub>R (Y axis) vs pK<sub>i</sub> CB<sub>2</sub>R (X axis) using the same scale and range for both axes (square plot). For each subset, the stereochemistry at the pendant amino acid residue is denoted in green (R) or orange (S). The plot also addresses the influence of the skeletal diversity (indoles or indazoles), represented as a circle or triangle (Fig. 7).

The presented data unequivocally confirmed that the (S) stereoisomers (green) are consistently more potent than the corresponding (R) stereoisomers (orange), with  $\Delta pK_i [pK_i(S) - pK_i(R)] > 2$  in most cases at both receptor subtypes. The difference in affinity between the (S) and (R) enantiomers seems to be more pronounced for indazole derivatives (when compared to their corresponding indole congeners).

Fig. 7 A evidences the (R) stereoisomers (orange triangles) are generally less affine (at both receptors) and slightly more affine towards CB<sub>2</sub>R (below the diagonal). Thus, some (R) stereoisomers of the ester series (**22i**, **23j**, **22o**, **23o**, **23m**) combine excellent affinity ( $K_i = 37.1$ ,  $14.7$ ,  $8.21$ ,  $1.20$ ,  $1.40$  nM) and an attractive selectivity (6–29 fold) toward CB<sub>2</sub>R. On the other hand, derivatives **23b** and **23d**, bearing (S) stereochemistry at R<sup>2</sup>, showed high CB<sub>2</sub>R affinity and somewhat subtype selectivity (8-fold). The selectivity trends noticed for the listed ligands can be also corroborated when comparing their functional data in CB<sub>1</sub>R and CB<sub>2</sub>R (Tables 1–4). The general SAR trends identified for ester

derivatives are reproduced within the amide subset (Fig. 7B), with most derivatives being highly affine at CB<sub>1</sub>R and CB<sub>2</sub>R and the (S) enantiomers (green) being systematically more affine than their correspondent (R) stereoisomers (orange). However, some amides show a slight preference for CB<sub>2</sub>R (**25d** and **24 h**), while derivatives **24 g** and **24 e** exhibit the opposite behavior, eliciting high affinity and superior selectivity towards CB<sub>1</sub>R. Like in the above cases, the above-mentioned trends can also be verified if we compare the functional data obtained for the listed ligands.

Fig. 8 was designed to evaluate the influence of the R<sup>2</sup> group (isopropyl or *tert*-butyl) on the binding affinity at CB<sub>1</sub>R and CB<sub>2</sub>R for esters or amides, and to calibrate the contribution of the scaffold (indole or indazole) and the stereodisposition (S or R). As in previous figures, the data was represented as a plot of pK<sub>i</sub> CB<sub>1</sub>R vs pK<sub>i</sub> CB<sub>2</sub>R, with the stereochemistry at the pendant amino acid residue denoted in green (R) or orange (S) and the heterocyclic core represented as a circle (indole) or triangle (indazole) (Fig. 8).

As observed, within the ester series (Fig. 8A), in general, *iso*-propyl derivatives seem to be slightly less affine (at both receptors) than *tert*-butyl analogues, particularly in the indole series. Within the indazole series the differences between *iso*-propyl or *tert*-butyl seem to be attenuated. A similar, but more accentuated, trend is observed when analyzing the influence of *iso*-propyl or *tert*-butyl groups in amide derivatives (Fig. 8B). Here, ligands bearing a *tert*-butyl group are consistently more affine than their *iso*-propyl analogues and this effect is more pronounced for the indazole series. Interestingly, within the amides of the (S) series carrying an indole core, a significant increase in affinity at both receptors can be observed when comparing a *tert*-butyl group with an *iso*-propyl group.

A bar plot was used to graphically evaluate the impact of R<sup>1</sup> (the tail of the SCRA structure) on the measured cannabinomimetic effect. In sharp contrast to the previous discussion (Figs. 6–8), attempts to generalize the influence of the group in R<sup>1</sup>, with the affinity measured in CB<sub>1</sub>R and CB<sub>2</sub>R, did not provide a clear trend (Fig. 9). As observed, most of the four derivatives in each subset (R<sup>1</sup> = pentyl, 5-F-pentyl, cyclohexylmethyl and 4-F-benzyl) elicited similar affinities. A possible explanation may lie in the fact that according to the proposed binding modes [4,5,7,19,22,

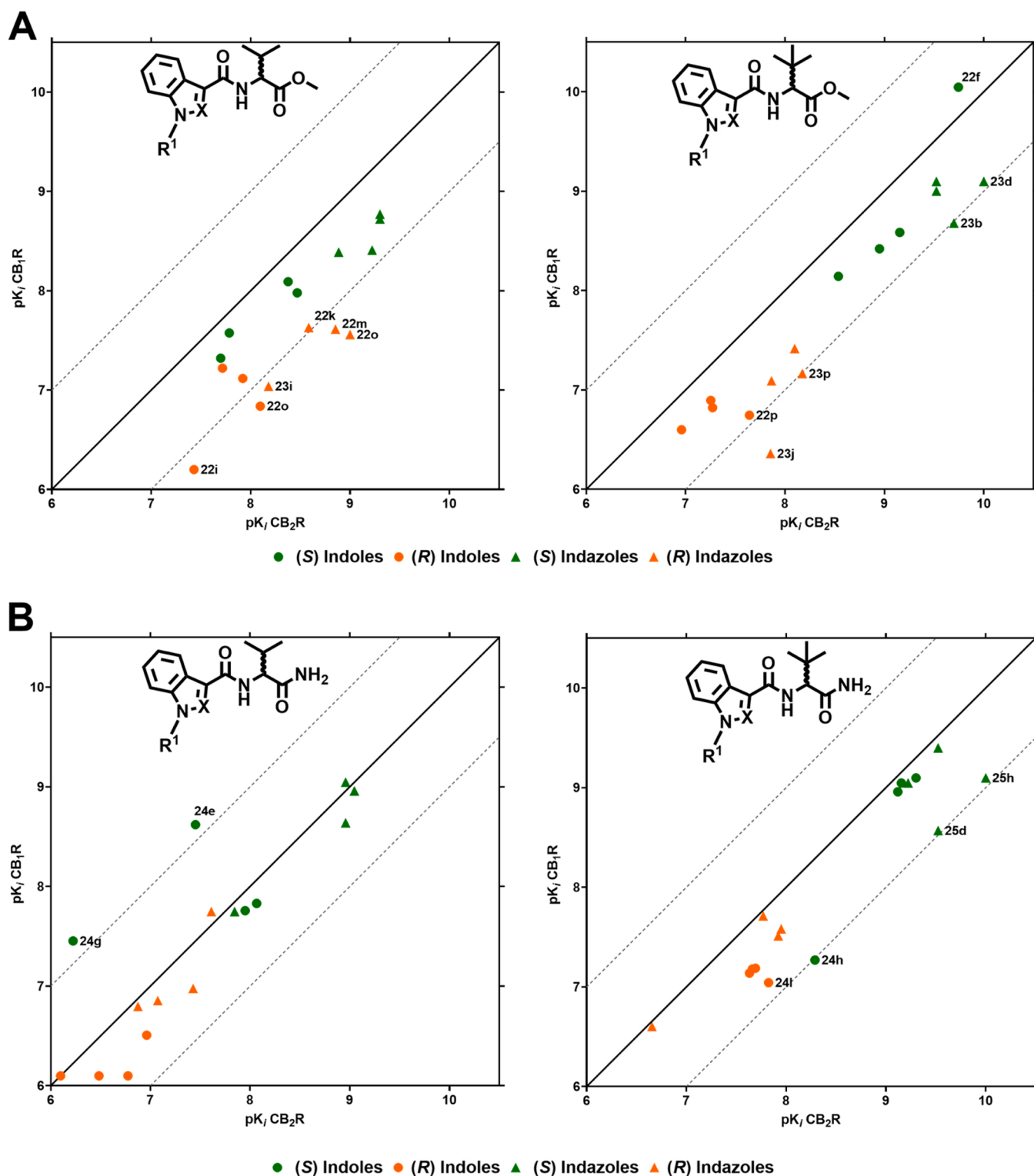


**Fig. 8.** Influence of the group at  $R^2$  on the cannabinomimetic profile. Affinity-selectivity plot for (S) (green) and (R) (orange) in the esters (**8A**) and amides (**8B**).

**23j**] for this class of ligands, at their respective orthosteric sites, this portion of the ligand allows for the greatest variation due to the large size of the hydrophobic pocket. [27,44].

Although the vast majority of the herein described ligands reproduce the intrinsic non-subtype-selective profile of SCRAs, examination of the large binding ( $pK_i$ ) data (Table 1–4) enabled the identification of novel derivatives that combine an attractive  $CB_2R$  affinity ( $K_i$  ranging 1.20 – 37.1 nM) and incipient selectivity towards  $CB_2Rs$  [e.g., compounds **22i**,

**22l** and **22o** (Table 1), **23j**, **23m** and **23o** (Table 2)]. Representative ligands exhibiting this profile are presented in Fig. 10. As observed, they contain an amino acid pendant residue bearing an ester group, either isopropyl or *tert*-butyl residues group at  $R^2$  and feature the (R) configuration within the stereocenter. As indicated above, the observed selectivity is modest, being more pronounced when comparing binding data (>10-fold) than functional data (>4-fold), and most derivatives in Fig. 10 retaining high affinity and potency at  $CB_1R$ .

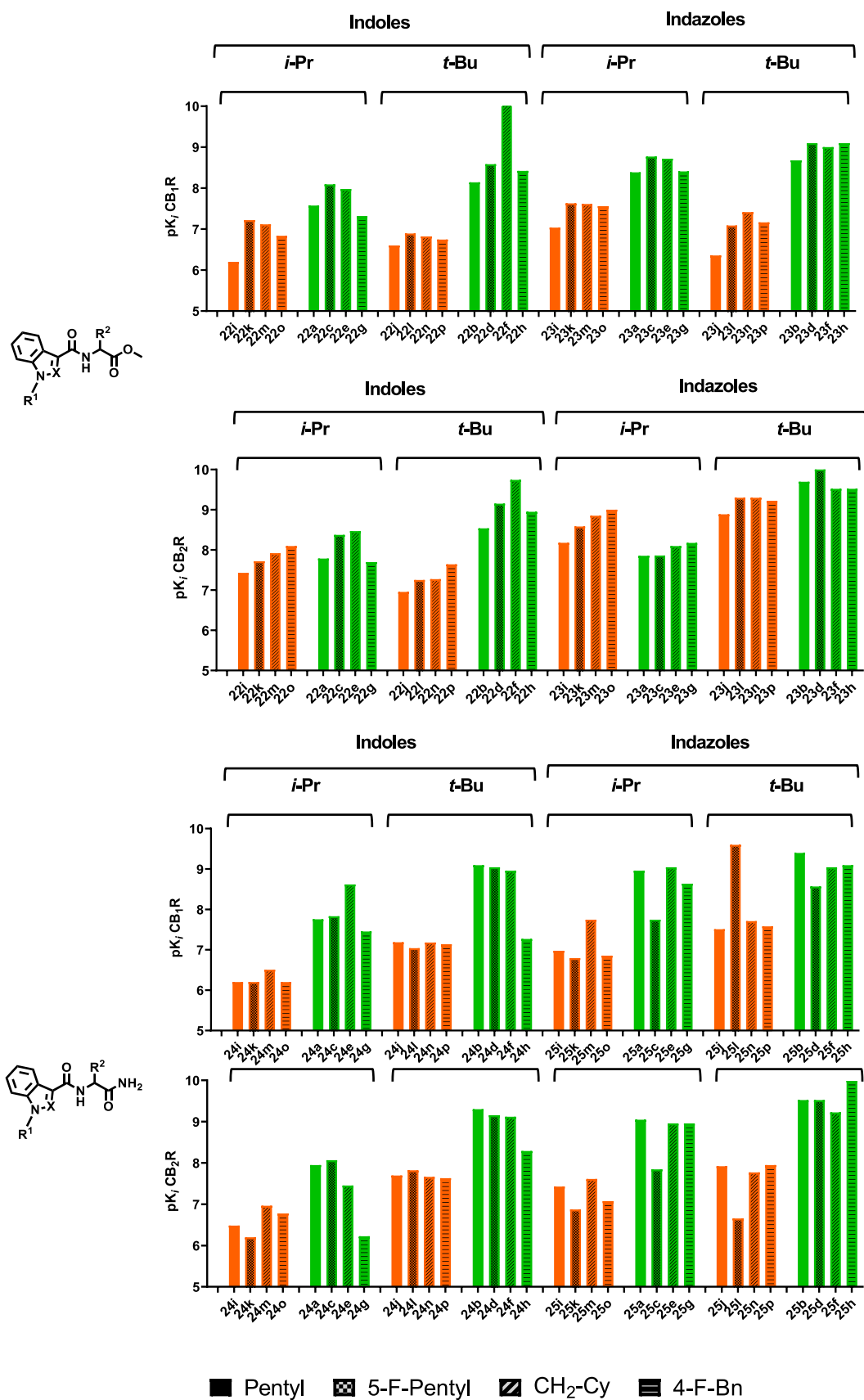


**Fig. 9.** Bar diagram evaluating the influence of the group at  $R^1$  on the cannabinomimetic profile in esters (9A) and amides (9B). Green bars correspond to (*S*) enantiomers and orange bars to (*R*) enantiomers.

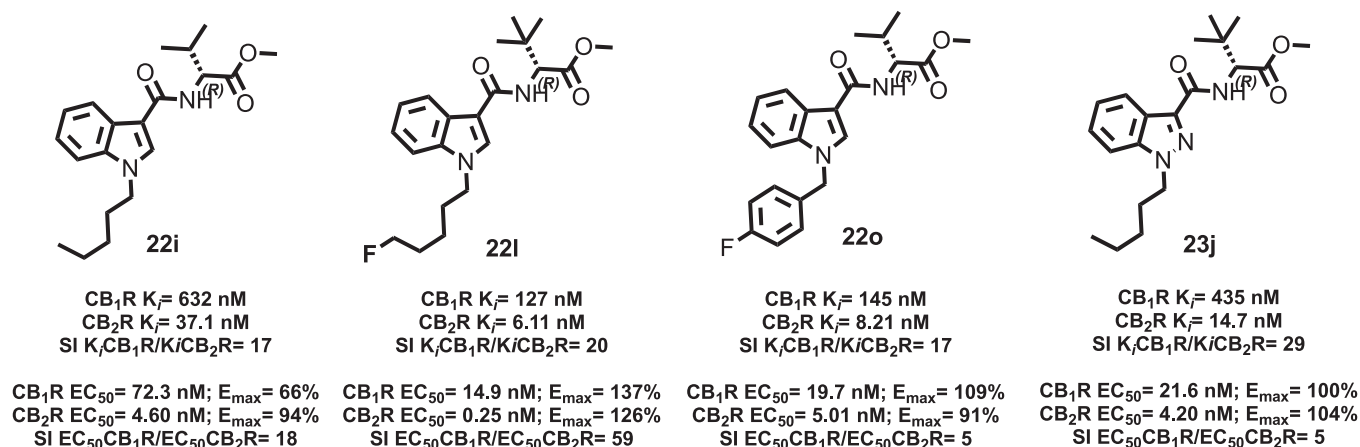


Fig. 10. Novel synthetic cannabinoid agonists eliciting incipient CB<sub>2</sub>R selective profile.

Among these derivatives, **22 l** and **22i** emerge as model ligands that show excellent efficacy, moderate and consistent sub-type selectivity towards CB<sub>2</sub>R in functional and affinity experiments. These ligands are currently being used in our programs to explore the significant, yet unrealized, therapeutic potential of CB<sub>2</sub>R activation. In contrast to previous studies, usually focusing on the characterization of drugs of abuse and small subsets, the library approach herein adopted has been instrumental in discovering CB<sub>2</sub>R agonists with incipient selectivity and identifying SAR trends that will inspire our ongoing program to develop CB<sub>2</sub>R agonists as anti-inflammatory, analgesic, and immunomodulatory therapeutics. [45,46] It must be noted that even though the ligands shown in Fig. 10 have modest selectivity and reveal structural features (*R* configuration) that inspire the design of new CB<sub>2</sub>R ligands, the inherent metabolic instability of SCRA esters and suboptimal physicochemical properties preclude their direct exploitation in drug discovery programs. Accordingly, functional derivatization using different pharmacomodulation strategies and physicochemical parameters optimization are currently being pursued in our laboratories.

### 3.5. Preliminary neurotoxicity study

The ever-changing structure of ligands in the illegal market makes it challenging to monitor abused SCRAs as well as to undertake systematic studies on their toxicological effects. Their high potency and excellent efficacy lead to lower doses being sufficient to obtain psychoactive effects. However, due to their unpredictable biological effects and unregulated and variable dosage and uses, overdose, intoxication and severe toxicity are more likely to occur. [47] With reports of intoxications and deaths following SCRAs use rapidly increasing, [48,49] toxicity studies are not only helpful in assessing the health threats associated with SCRAs abuse, but also in proposing appropriate medical management for cases of intoxication arising from SCRA consumption. [50–52] Although case reports and retrospective studies of acute intoxication by SCRAs confirm that they cause severe effects (e.g., seizures, cardiovascular damage, kidney damage, stroke psychosis, paranoia, anxiety attacks), [47,50,52,53] little is currently known about the mechanisms by which these structures exert toxic effects. [53] Several reports have assessed the toxicity of commonly abused SCRAs evidencing remarkable harmful effects. Noteworthy, growing scientific evidence highlights that SCRAs consume alters psychoactive and cognitive responses. [11,54] However, the cytotoxicity of known SCRAs (and emerging derivatives) in mammalian neuronal cells remains scarcely explored. [55].

In the context of this study, we decided to preliminarily examine the neurotoxicity signatures of a subset of herein prepared synthetic cannabinoid agonists in primary mouse neuronal cells. The selected ligands included well-known SCRAs [22c (5 F-MDMB-PICA), 22e (MMB-

CHMICA), 22 f (MDMB-CHMICA), 22 h (MDMB-FUBICA), 23e (AMB-CHMINACA), 23 f (MDMB-CHMINACA), 23 h (MDMB-FUBINACA), 24d (5-F-AD-BICA), 24e (AB-CHMICA), 24 f (ADB-CHMICA), 24 g (AB-FUBICA), 25d (5-FADB-PINACA), 25e (AD-CHMINACA), 25 f (ABD-CHMINACA), 25 h (ADB-FUBINACA)] as well as four hitherto untapped derivatives [(*R*) stereoisomers, 22 m, 23 m, 24 n, 25 n] all of them being representatives of the structural diversity explored within the study. As the enantiomers (*R*) showed generally lower potency and efficacy compared to their congeners (*S*), for this preliminary exploration it was decided to prioritize the latter subset (*S*). Fig. 11 represents the results of the neuronal toxicity of selected ligands, evaluated at 100 nM in mouse primary neuronal cells.

A first inspection of the generated data (Fig. 11) reveals that, in a clear contrast to the effect measured for  $\Delta^9$ -THC and CBD, all ligands significantly reduced cell viability (typically from 30% to 70%). The reduction in cell viability seems to be functional and scaffold dependent, with amides derived of the indazole core (Fig. 11, compounds 25) eliciting superior neurotoxicity. Whereas the observed toxicity profiles could be consequence of different features (e.g., pharmacological, and pharmacokinetic), a first analysis of the structural relationship among the selected ligands enables the ascertaining of similarities and/or differences that could be potentially affecting the observed neurotoxicity signatures. Thus, indole ester derivatives seem to be slightly less cytotoxic than their indazole analogues (Fig. 11, compare 22e and 23e, 22 f and 23 f, 22 h and 23 h). Such a trend is considerably more pronounced in the amide series, with indole amides being clearly less cytotoxic than their corresponding analogues in the indazole series (Fig. 11, compare 24d and 25d, 24e and 25e, 24 f and 25 f). Although the limited number of derivatives with stereochemistry (*R*) in the pendant amino acid chain studied precludes reaching definitive conclusions, the obtained data suggest that, except for 24 n, these derivatives generally exhibit superior neurotoxicity. Indeed, the ligand exhibiting superior neuronal toxicity (25 n) is an indazole amide bearing a *tert*-butyl group with (*R*) configuration on the pendant amino acid chain. These preliminary results suggest that special attention and control should be paid to the possible emergence on the illicit market of SCRAs based on an indazole core and containing an amide group. Further studies are currently being conducted in our laboratories to complete the pharmacological characterization and broaden the toxicity analysis of this large collection of SCRAs.

## 4. Conclusions

SCRAs are designer drugs that mimic the effects of  $\Delta^9$ -THC and pose a serious threat to public health and require effective collaboration between the scientific and law enforcement communities. Herein we reported the functional and binding data of the largest and most diverse



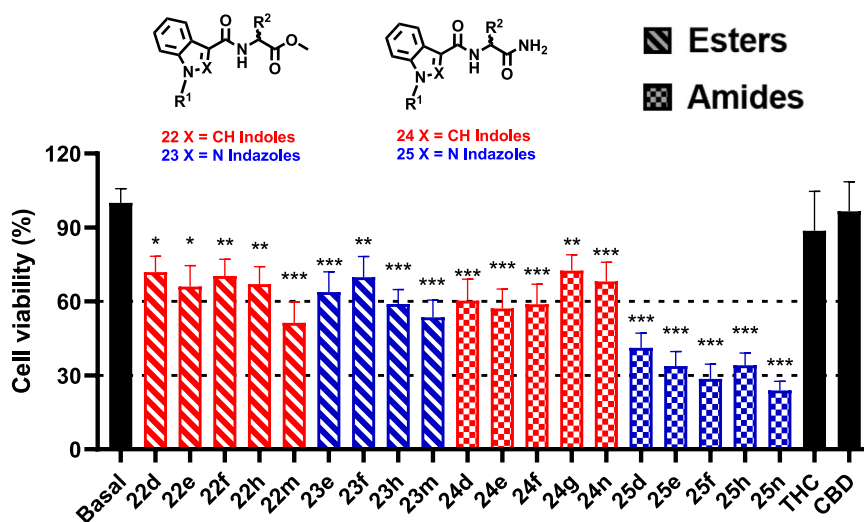


Fig. 11. Neuronal toxicity of representative SCRA derivatives (100 nM) in mouse primary neuronal cells.

collection of SCRA derivatives published to date. Our results revealed the cannabimimetic profile of 14 novel derivatives that could be (or may currently be) used as illegal psychoactive substances. Comparative analysis of the affinity data provided emerging SAR and SSR trends and identified some CB<sub>2</sub>R selective ligands, while a preliminary study in primary neuronal cells evidenced an eventual neurotoxicity of SCRA derivatives. The library constitutes a collaborative tool to address some of the challenges posed by the market for new psychoactive substances.

#### CRedit authorship contribution statement

**Claudia Gioé-Gallo:** Investigation, Validation, Writing – original draft. **Sandra Ortigueira:** Investigation, Validation. **José Brea:** Investigation, Validation. **Iu Raich:** Investigation, Validation. **Johnny Azuaje:** Methodology, Investigation, Validation. **M. Rita Paleo:** Methodology, Investigation, Validation, Supervision. **Maria Majellaro:** Investigation, Validation, Writing – original draft. **María Isabel Loza:** Validation, Funding acquisition. **Cristian O. Salas:** Methodology, Validation. **Xerardo García-Mera:** Methodology, Investigation, Validation. **Gemma Navarro:** Methodology, Investigation, Validation. **Eddy Sotelo:** Conceptualization, Supervision, Funding acquisition, Writing – review & editing.

#### Declaration of Competing Interest

The authors declare the following financial interests/personal relationships which may be considered as potential competing interests: EDDY SOTELO reports was provided by Government of Galicia.

#### Acknowledgments

This work was financially supported by the Consellería de Cultura, Educación e Ordenación Universitaria of the Galician Government: (grant: ED431B 2020/43), Centro Singular de Investigación de Galicia accreditation 2019–2022 (ED431G 2019/03), Ministerio de Ciencia e Innovación (PID2020-113430RB-I00) and the European Regional Development Fund (ERDF).

#### Appendix A. Supporting information

Supplementary data associated with this article can be found in the online version at [doi:10.1016/j.biopha.2023.114934](https://doi.org/10.1016/j.biopha.2023.114934).

#### References

- [1] UNODC. Early warning advisory on new psychoactive substances (<https://www.unodc.org/LSS/Page/NPS>).
- [2] A. Shafi, A.J. Berry, H. Sumnall, D.M. Wood, D.K. Tracy, New psychoactive substances: a review and updates, *Ther. Adv. Psychopharmacol.* 10 (2020), 204512532096719.
- [3] F. Zapata, J.M. Matey, G. Montalvo, C. García-Ruiz, Chemical classification of new psychoactive substances (NPS), *Microchem. J.* (2021) 163.
- [4] V. Abbate, M. Schwenk, B.C. Presley, N. Uchiyama, The ongoing challenge of novel psychoactive drugs of abuse. Part I. Synthetic cannabinoids (IUPAC Technical Report), *Pure Appl. Chem.* 90 (2018) 1255–1282.
- [5] S.D. Banister, M. Connor, The chemistry and pharmacology of synthetic cannabinoid receptor agonists as new psychoactive substances: origins, *Handb. Exp. Pharm.* 252 (2018) 165–190.
- [6] D. Abdulrahim, O. Bowden-Jones, Harms of synthetic cannabinoid receptor agonists (SCRA) and their management, *Nov. Psychoact. Treat. UK Netw.* 2015 (2016) 25.
- [7] C.T. Schoeder, C. Hess, B. Madea, J. Meiler, C.E. Müller, Pharmacological evaluation of new constituents of “spice”: synthetic cannabinoids based on indole, indazole, benzimidazole and carbazole scaffolds, *Forensic Toxicol.* 36 (2018) 385–403.
- [8] C. Hess, C.T. Schoeder, T. Pillaiyar, B. Madea, C.E. Müller, Pharmacological evaluation of synthetic cannabinoids identified as constituents of spice, *Forensic Toxicol.* 34 (2016) 329–343.
- [9] A.J. Adams, S.D. Banister, L. Irizarry, J. Trecki, M. Schwartz, R. Gerona, “Zombie” outbreak caused by the synthetic cannabinoid AMB-FUBINACA in New York, *New Engl. J. Med.* 376 (2017) 235–242.
- [10] W. Hourani, S.P.H. Alexander, Cannabinoid ligands, receptors and enzymes: pharmacological tools and therapeutic potential, *Brain Neurosci. Adv.* 2 (2018), 239821281878390.
- [11] K. Cohen, A.M. Weinstein, Synthetic and non-synthetic cannabinoid drugs and their adverse effects—a review from public health perspective, *Front. Public Health* 6 (2018) 13–16.
- [12] M.H. Deventer, Van Uytendange, K. Vinckier, I.M.J. Renier, F. Guillou, C. Stove, C. P. A new cannabinoid receptor 1 selective agonist evading the 2021 “China Ban”: ADB-FUBIATA, *Drug Test. Anal.* 14 (2022) 1639–1644.
- [13] R. Fredriksson, M.C. Lagerström, L.G. Lundin, H.B. Schiöth, The G-protein-coupled receptors in the human genome form five main families. phylogenetic analysis, paralogon groups, and fingerprints, *Mol. Pharmacol.* 63 (2003) 1256–1272.
- [14] A.C. Howlett, F. Barth, T.I. Bonner, G. Cabral, P. Casellas, W.A. Devane, C. C. Felder, M. Herkenham, K. Mackie, B.R. Martin, R. Mechoulam, R.G. Pertwee, International union of pharmacology. XXVII. Classification of cannabinoid receptors, *Pharmacol. Rev.* 54 (2002) 161–202.
- [15] C.H. Ashton, Pharmacology and effects of cannabis: a brief review, *Br. J. Psychiatry* 178 (2001) 101–106.
- [16] G.A. Cabral, E.S. Raborn, L. Griffin, J. Dennis, F. Marciano-Cabral, CB 2 receptors in the brain: role in central immune function, *Br. J. Pharmacol.* 153 (2008) 240–251.
- [17] A.M. Miller, N. Stella, CB 2 receptor-mediated migration of immune cells: it can go either way, *Br. J. Pharmacol.* 153 (2008) 299–308.
- [18] C. Turcotte, M.R. Blanchet, M. Laviolette, N. Flamand, The CB2 receptor and its role as a regulator of inflammation, *Cell. Mol. Life Sci.* 73 (2016) 4449–4470.
- [19] C. Liu, W. Jia, Z. Hua, Z. Qian, Identification and analytical characterization of six synthetic cannabinoids NNL-3, 5F-NPB-22-7 N, 5F-AKB-48-7 N, 5F-EDMB-PINACA, EMB-FUBINACA, and EG-018, *Drug Test. Anal.* 9 (2017) 1251–1261.

- [20] M. Longworth, S.D. Banister, R. Boyd, R.C. Kevin, M. Connor, I.S. McGregor, M. Kassiou, Pharmacology of cumyl-carboxamide synthetic cannabinoid new psychoactive substances (NPS) CUMYL-BICA, CUMYL-PICA, CUMYL-5F-PICA, CUMYL-5F-PINACA, and their analogues, *ACS Chem. Neurosci.* 8 (2017) 2159–2167.
- [21] S.D. Banister, M. Longworth, R. Kevin, S. Sachdev, M. Santiago, J. Stuart, J.B. C. Mack, M. Glass, I.S. McGregor, M. Connor, M. Kassiou, Pharmacology of valinate and tert-leucinate synthetic cannabinoids 5F-AMBICA, 5F-AMB, 5F-ADB, AMB-FUBINACA, MDMB-FUBINACA, MDMB-CHMICA, and their analogues, *ACS Chem. Neurosci.* 7 (2016) 1241–1254.
- [22] R. Santos-Toscano, A. Guirguis, C. Davidson, How preclinical studies have influenced novel psychoactive substance legislation in the UK and Europe, *Br. J. Clin. Pharmacol.* 86 (2020) 452–481.
- [23] R. Le Boisselier, J. Alexandre, V. Lelong-Boulouard, D. Debruyne, Focus on cannabinoids and synthetic cannabinoids, *Clin. Pharmacol. Ther.* 101 (2017) 220–229.
- [24] S.D. Banister, M. Moir, J. Stuart, R.C. Kevin, K.E. Wood, M. Longworth, S. M. Wilkinson, C. Beinat, A.S. Buchanan, M. Glass, M. Connor, I.S. McGregor, M. Kassiou, Pharmacology of Indole and Indazole Synthetic Cannabinoid Designer Drugs AB-FUBINACA, ADB-FUBINACA, AB-PINACA, ADB-PINACA, 5F-AB-PINACA, 5F-ADB-PINACA, ADBICA, and 5F-ADBICA, *ACS Chem. Neurosci.* 6 (2015) 1546–1559.
- [25] A. Cannaeert, E. Sparkes, E. Pike, J.L. Luo, A. Fang, R.C. Kevin, R. Ellison, R. Gerona, S.D. Banister, C.P. Stove, Synthesis and in vitro cannabinoid receptor 1 activity of recently detected synthetic cannabinoids 4F-MDMB-BICA, 5F-MPP-PICA, MMB-4en-PICA, CUMYL-CBMICA, ADB-BINACA, APP-BINACA, 4F-MDMB-BINACA, MDMB-4en-PINACA, A-CHMINACA, 5F-AB-P7AICA, 5F-MDMB-P7AICA, *An. ACS Chem. Neurosci.* 11 (2020) 4434–4446.
- [26] I.P. Buchler, M.L.J. Hayes, S.G. Hegde, S.L. Hockerman, D.E. Jones, S.W. Kortum, J. G. Rico, R.E. Tenbrink, K.K. Wu, Indazole derivatives WO 2009106980 A2 2009.
- [27] K. Krishna Kumar, M. Shalev-Benami, M.J. Robertson, H. Hu, S.D. Banister, S. A. Hollingsworth, N.R. Latorra, H.E. Kato, D. Hilger, S. Maeda, W.I. Weis, D. L. Farrens, R.O. Dror, S.V. Malhotra, B.K. Kobilka, G. Skiniotis, Structure of a signaling cannabinoid receptor 1-G protein complex, *Cell* 176 (448–458) (2019), e12.
- [28] I. Lastres-Becker, F. Molina-Holgado, J.A. Ramos, R. Mechoulam, J. Fernández-Ruiz, Cannabinoids Provide Neuroprotection against 6-Hydroxydopamine Toxicity in Vivo and in Vitro: relevance to Parkinson's Disease, *Neurobiol. Dis.* 19 (2005) 96–107.
- [29] T. Doi, A. Asada, A. Takeda, T. Tagami, M. Katagi, H. Kamata, Y. Sawabe, Enantioseparation of the carboxamide-type synthetic cannabinoids N-(1-Amino-3-Methyl-1-Oxobutan-2-yl)-1-(5-Fluoropentyl)-1H-Indazole-3-Carboxamide and methyl [1-(5-Fluoropentyl)-1H-Indazole-3-Carbonyl]-valinate in illicit herbal products, *J. Chromatogr. A* 1473 (2016) 83–89.
- [30] L.H. Antonides, A. Cannaeert, C. Norman, L. Vives, A. Harrison, A. Costello, N. N. Daeid, C.P. Stove, O.B. Sutcliffe, C. McKenzie, Enantiospecific synthesis, chiral separation, and biological activity of four indazole-3-carboxamide-type synthetic cannabinoid receptor agonists and their detection in seized drug samples, *Front. Chem.* 7 (2019) 1–20.
- [31] M. Patel, J.J. Manning, D.B. Finlay, J.A. Javitch, S.D. Banister, N.L. Grimsey, M. Glass, Signalling profiles of a structurally diverse panel of synthetic cannabinoid receptor agonists, *Biochem. Pharmacol.* 175 (2020), 113871.
- [32] E. Wouters, J. Walraed, M.J. Robertson, M. Meyrath, M. Szpakowska, A. Chevigné, G. Skiniotis, C. Stove, Assessment of biased agonism among distinct synthetic cannabinoid receptor agonist scaffolds, *ACS Pharmacol. Transl. Sci.* 3 (2020) 285–295.
- [33] G. Navarro, A. Cordero, M. Brugarolas, E. Moreno, D. Aguinaga, L. Pérez-Benito, S. Ferre, A. Cortés, V. Casadó, J. Mallol, E.I. Canela, C. Lluís, L. Pardo, P. J. McCormick, R. Franco, Cross-communication between Gi and Gs in a G-protein-coupled receptor heterotetramer guided by a receptor C-terminal domain, *BMC Biol.* 16 (2018) 1–15.
- [34] J. Hradsky, V. Raghuram, P.P. Reddy, G. Navarro, M. Hupe, V. Casado, P. J. McCormick, Y. Sharma, M.R. Kreutz, M. Mikhaylova, Post-translational membrane insertion of tail-anchored transmembrane EF-hand Ca<sup>2+</sup>-sensor calneurons requires the TRC40/Asn1 protein chaperone, *J. Biol. Chem.* 286 (2011) 36762–36776.
- [35] G. Navarro, S. Ferré, A. Cordero, E. Moreno, J. Mallol, V. Casadó, A. Cortés, H. Hoffmann, J. Ortiz, E.I. Canela, C. Lluís, L. Pardo, R. Franco, A.S. Woods, Interactions between Intracellular Domains as Key Determinants of the Quaternary Structure and Function of Receptor Heteromers, *J. Biol. Chem.* 285 (2010) 27346–27359.
- [36] R. Williams, T.H. Sellors, Particularly 788 (1977) 1977.
- [37] F. Caputo, S. Corbetta, O. Piccolo, D. Vigo, Seeking for selectivity and efficiency: new approaches in the synthesis of raltegravir, *Org. Process Res. Dev.* 24 (2020) 1149–1156.
- [38] J.R. Lakowicz, Principles of Fluorescence Spectroscopy, 3rd Principles of Fluorescence Spectroscopy, third ed., 2006, Springer, New York, USA, 2006.
- [39] N. Berova, K. Nakanishi, R.W. Woody, Circular Dichroism - Principles and Applications, John Wiley & Sons, 2000.
- [40] S. Eto, M. Yamaguchi, M. Bounoshita, T. Mizukoshi, H. Miyano, High-throughput comprehensive analysis of d- and l-amino acids using ultra-high performance liquid chromatography with a circular dichroism (CD) detector and its application to food samples, *J. Chromatogr. B Anal. Technol. Biomed. Life Sci.* 879 (2011) 3317–3325.
- [41] A.L. Jenkins, W.A. Hedgepeth, Analysis of chiral pharmaceuticals using HPLC with CD detection, *Chirality* 17 (2005) 24–29.
- [42] M. Fujioaka, N. Omori, Subtleties in GPCR drug discovery: a medicinal chemistry perspective, *Drug Discov. Today* 17 (2012) 1133–1138.
- [43] J. Markham, E. Sparkes, R. Boyd, S. Chen, J.J. Manning, D. Finlay, F. Lai, E. McGregor, C.J. Maloney, R.R. Gerona, M. Connor, I.S. McGregor, D.E. Hibbs, M. Glass, R.C. Kevin, S.D. Banister, Defining steric requirements at CB1 and CB2 cannabinoid receptors using synthetic cannabinoid receptor agonists 5F-AB-PINACA, 5F-ADB-PINACA, PX-1, PX-2, NNL-1, and their analogues, *ACS Chem. Neurosci.* 13 (2022) 1281–1295.
- [44] X. Li, T. Hua, K. Vemuri, J.H. Ho, Y. Wu, L. Wu, P. Popov, O. Benchama, N. Zvonok, K. Locke, L. Qu, G.W. Han, M.R. Iyer, R. Cinar, N.J. Coffey, J. Wang, M. Wu, V. Katritch, S. Zhao, G. Kunos, L.M. Bohn, A. Makriyannis, R.C. Stevens, Z.J. Liu, Crystal Structure of the Human Cannabinoid Receptor CB2, *Cell* 176 (2019) 459–467, e13.
- [45] M. Aghazadeh Tabrizi, P.G. Baraldi, P.A. Borea, K. Varani, Medicinal chemistry, pharmacology, and potential therapeutic benefits of cannabinoid CB2 receptor agonists, *Chem. Rev.* 116 (2016) 519–560.
- [46] F. Spinelli, E. Capparelli, C. Abate, N.A. Colabufo, M. Contino, Perspectives of cannabinoid type 2 receptor (CB2R) ligands in neurodegenerative disorders: structure-affinity relationship (SAfR) and structure-activity relationship (SAR) studies, *J. Med. Chem.* 60 (2017) 9913–9931.
- [47] R.J. Tait, D. Caldicott, D. Mountain, S.L. Hill, S. Lenton, A systematic review of adverse events arising from the use of synthetic cannabinoids and their associated treatment, *Clin. Toxicol.* 54 (2016) 1–13.
- [48] Jordan Trecki Ph.D., Roy R. Gerona Ph.D., Michael D. Schwartz M.D., Synthetic Cannabinoid-Related Illnesses and Deaths, *N. Engl. J. Med.* 373 (2015) 103–107.
- [49] N. Hussain, F. Hussain, D. Haque, S. Saeed, R. Jesudas, An Outbreak of Brodifacoum Coagulopathy Due to Synthetic Marijuana in Central Illinois, *Mayo Clin. Proc.* 93 (2018) 957–958.
- [50] A. Alipour, P.B. Patel, Z. Shabbir, S. Gabrielson, Review of the many faces of synthetic cannabinoid toxicities, *Ment. Health Clin.* 9 (2019) 93–99.
- [51] J. Alexandre, R. Malheiro, D.D. Silva, H. da; Carmo, F. Carvalho, J.P. Silva, The synthetic cannabinoids Thj-2201 and 5f-Pb22 enhance in vitro Cb1 receptor-mediated neuronal differentiation at biologically relevant concentrations, *Int. J. Mol. Sci.* 21 (2020) 1–22.
- [52] Y. Sezer, A.T. Jannuzzi, M.A. Huestis, B. Alpertunga, In vitro assessment of the cytotoxic, genotoxic and oxidative stress effects of the synthetic cannabinoid JWH-018 in human SH-SY5Y neuronal cells, *Toxicol. Res.* 9 (2020) 734–740.
- [53] D.B. Finlay, J.J. Manning, M.S. Ibsen, C.E. Macdonald, M. Patel, J.A. Javitch, S. D. Banister, M. Glass, Do toxic synthetic cannabinoid receptor agonists have signature in vitro activity profiles? A case study of AMB-FUBINACA, *ACS Chem. Neurosci.* 10 (2019) 4350–4360.
- [54] R.M. Murray, H. Quigley, D. Quattrone, A. Englund, M. Di Forti, Traditional marijuana, high-potency cannabis and synthetic cannabinoids: increasing risk for psychosis, *World Psychiatry* 15 (2016) 195–204.
- [55] K. Tomiyama, M. Funada, Cytotoxicity of synthetic cannabinoids on primary neuronal cells of the forebrain: the involvement of cannabinoid CB1 receptors and apoptotic cell death, *Toxicol. Appl. Pharmacol.* (2013).